IEEE Access
Multidisciplinary ⋮ Rapid Review ⋮ Open Access Journal

Received April 8, 2019, accepted April 29, 2019, date of publication May 7, 2019, date of current version May 21, 2019.

Digital Object Identifier 10.1109/ACCESS.2019.2915375

On Performance of Hexagonal, Cross, and Rectangular QAM for Multi-Relay Systems

PRAVEEN K. SINGYA[1], (Student Member, IEEE), NAGENDRA KUMAR[2], (Member, IEEE), VIMAL BHATIA[1], (Senior Member, IEEE), AND MOHAMED-SLIM ALOUINI[3], (Fellow, IEEE)

[1]Discipline of Electrical Engineering, IIT Indore, Indore 453552, India
[2]Department of Electronics and Communication Engineering, National Institute of Technology, Jamshedpur 831014, India
[3]Computer, Electrical, and Mathematical Science and Engineering Division, King Abdullah University of Science and Technology, Thuwal 23955-6900, Saudi Arabia

Corresponding author: Praveen K. Singya (phd1501102023@iiti.ac.in)

This work is partially supported by the Ministry of Electronics and Information Technology Research and Development Work, Government of India, through the Visvesvaraya Ph.D. Scheme being implemented by Digital India Corporation.

ABSTRACT Error performance is considered as one of the most important performance measures, and deriving the closed-form expressions for efficient modulation techniques over generalized fading channels is important for future cellular systems. In this paper, the performance of a dual-hop amplify-and-forward multi-relay system with best relay selection is analyzed over independent and non-identically distributed (i.n.i.d.) Nakagami-m fading links with both integer and non-integer fading parameters. The impact of practical constraints of imperfect channel state information (CSI) and non-linear power amplifier (NLPA) at each of the relays are considered. Closed-form expressions for the outage probability are derived for both integer and non-integer fading parameters, and asymptotic analysis on the outage probability is performed to obtain the diversity order of the considered multi-relay system. Based on the cumulative distribution function approach, average symbol error rate (ASER) expressions for general order hexagonal QAM, general order rectangular QAM, and 32-cross QAM schemes are also derived. The comparative analysis of ASER for various QAM schemes with different constellations is also illustrated. Furthermore, the impact of the number of relays, fading parameter, channel estimation error, and non-linear distortion on the system performance is also highlighted. Finally, the derived analytical results are validated through Monte-Carlo simulations.

INDEX TERMS Nakagami-m, multi-relay, imperfect CSI, non-linear power amplifier (NLPA), hexagonal QAM (HQAM), rectangular QAM (RQAM), cross QAM (XQAM).

I. INTRODUCTION

Cooperative communication has gained enormous attention in current and future wireless systems due to its improved spectral efficiency, enhanced coverage and link capacity. Cooperative relaying has been considered in IEEE 802.16j/m, 3GPP LTE-Advanced and can be viewed as a promising solution for 5G and beyond systems [1]. To exploit the advantages of relaying systems, there are various relaying schemes such as amplify-and-forward (AF), decode-and-forward (DF) and compress-and-forward (CF), amongst which AF is preferred due to its low cost, easy deployment and low signal processing resources requirement. Further, the statistical behavior of the wireless links is characterized by independent and non-identically distributed (i.n.i.d.) Nakagami-m fading which is a versatile channel model and is used to model variety of fading environments such as single sided Gaussian distribution ($m = 1/2$) and Rayleigh distribution ($m = 1$) as its special cases. It can closely approximate the Hoyt and Rician distributions, and is also suitable for characterizing channel fading worse than Rayleigh fading ($0.5 \leq m < 1$) [2].

Further, adaptive transmission has become important scheme in present and future wireless communication systems due to adaptive modulation and coding, and optimum power utilization is adopted in many applications such as digital broadcasting over cable line, high definition TV (HDTV) broadcasting services, telephone line modems due to its increased data throughput and spectral efficiency [3]. Thus, for optimum utilization of limited bandwidth, adaptive usage

The associate editor coordinating the review of this manuscript and approving it for publication was Yuan Gao.

of different modulation schemes is mandatory for system's efficiency and economy.

Hence, for further data-rate enhancement with optimum spectral efficiency, higher order modulation techniques such as the family of quadrature amplitude modulations (QAM) (i.e. squared QAM (SQAM), rectangular QAM (RQAM), cross QAM (XQAM) and hexagonal QAM (HQAM)) have gained increased attention due to their high power and bandwidth efficiency. RQAM is a versatile modulation scheme due to the inclusion of SQAM, orthogonal binary frequency shift keying (OBFSK), quadrature phase shift keying (QPSK) and multi-level amplitude shift keying (ASK) as its special cases. RQAM is efficiently used in various applications such as high speed mobile communication systems, telephone-line modems, microwave communications, asymmetric subscriber loop etc [2]. However, for odd number of constellation points, RQAM is not a good choice and an optimum XQAM constellation is preferred due to its lower peak and average power. The XQAM constellation is formed by modifying the RQAM constellation with the removal of outer corner points and arranging them such that the peak and average power of the constellation is reduced. With this, XQAM provides at-least 1 dB SNR gain over RQAM scheme [4]. XQAM scheme has been adopted in different practical systems such as XQAM constellations with 5-15 bits are preferred in asymmetric digital subscriber line (ADSL) and very high bit-rate digital subscriber line (VDSL). Further, 32-XQAM and 128-XQAM are preferred in digital video broadcasting-cable (DVB-C) [5]. The increasing demand for high-data rates directs towards the formation of optimum two dimensional (2D) hexagonal lattice based constellation which is referred as HQAM. HQAM has the densest 2D packing with optimum Euclidean distance between the points even for the higher order constellations with lower peak to average power ratio (PAPR) and provides considerable SNR gain over the other QAM schemes [6]–[8].

A. RELATED WORK

In the literature, considerable work on the average symbol error rate (ASER) performance of various QAM schemes has been reported [2], [6], [8]–[14] for different wireless relaying or non-relaying systems over various fading scenarios with perfect channel state information (CSI).

In [2], exact ASER expressions of RQAM, $\pi/4$-QPSK and differentially encoded QPSK (De-QPSK) are derived for a non-relaying multi-branch selection combining (SC) receiver system over i.n.i.d. Nakagami-m fading channels. For a multi-relay system, closed-form expressions of ASER for HQAM, XQAM, RQAM, $\pi/4$-QPSK and De-QPSK are derived in [6] over i.n.i.d. Nakagami-m fading channels. In [10], bit error rate (BER) performance of hierarchical QAM constellations is analyzed. For this, generic exact expressions of BER for the 4/M-QAM (square and rectangular) constellations are derived over the additive white Gaussian noise (AWGN) channel. In [11], closed-form expressions of ASER for RQAM and XQAM schemes are derived for a dual-hop DF relaying system over $\eta-\mu$ and $\kappa-\mu$ fading channels. In [12], closed-form expressions of ASER for various M-ary QAM and phase shift keying (PSK) schemes, and channel capacity are derived for a non-relaying multi branch system with SC receiver over independent and identically distributed (i.i.d.) $\eta-\mu$ channels. In [13], symbol error probability (SEP) expression for general order HQAM scheme is derived for a non-relaying system over Rayleigh distributed channel. In [14], ASER performance of triangular QAM (TQAM) (special case of HQAM) is analyzed for a non-relaying system over AWGN channel.

In practice, perfect knowledge of CSI at all the communication nodes is not feasible, which introduces channel estimation error (CEE) at the nodes. CEE has significant detrimental impact on the system performance which cannot be ignored [15], [16]. Thus, over the years, researchers have also analyzed the impact of CEE on various relaying systems. In [7], closed-form expressions for the outage probability, asymptotic outage probability and ASER of HQAM and RQAM schemes are derived for a single relay AF network over i.n.i.d. Nakagami-m fading links with imperfect CSI. In [17], performance analysis of an AF multi-relay system with selection cooperation is shown over Rayleigh distributed channel with imperfect CSI. For a two-way AF relaying system, finite-SNR diversity-multiplexing trade-off over Nakagami-m fading channels with imperfect CSI is shown in [18]. In [19], for a fixed-gain single and opportunistic AF relaying system, accurate SEP expressions of M-ary PSK over Rayleigh fading channels with imperfect CSI are derived. In [20], power allocation and relay selection for an AF multi-relay system with imperfect CSI are investigated.

While moving towards 5G and beyond systems, with the increased multimedia applications through wireless channels, the bandwidth requirement has increased. This increased bandwidth requirement makes the design of a linear power amplifier (PA) very difficult. In cooperative relaying, high PAPR occurs not only in uplink but also in downlink due to the presence of non-linear PA (NLPA) at relays[1] which introduces significant non-linear distortion (NLD) in the received signal. Therefore, studying the impact of NLD on the system performance is important from perspective of system design. Thus, researchers have also observed the impact of NLD on the performance of various cooperative relaying systems [21]–[27].

In [22], performance of a single relay AF orthogonal frequency division multiplexing (OFDM) system is analyzed for maximum ratio combining (MRC) receiver over i.n.i.d. Nakagami-m fading links with NLPA at the relay. For a multi-relay AF OFDM system, closed-form expressions for the outage probability and ASER of RQAM scheme are derived in [23] by considering NLPA at the relays. In [24], performance of a single relay AF OFDM system is analyzed for SC and MRC receivers over Rayleigh distributed links

[1] In general, relays are small units like user equipments which have less signal processing resources.

by considering an NLPA at the relay. In [25], for a two-way non-linear fixed and variable gain single AF relay system, closed-form expressions of the outage probability are derived over Rayleigh fading channels. For a multi-relay AF OFDM system with SC receiver, closed-form expressions of outage probability, asymptotic outage probability and ASER of SQAM scheme are derived in [26] with NLPA at relays.

For the first time, combined impact of the outdated CSI and NLD have been observed in [27] on relaying system. In [27], impact of NLD of high PA (with different PA models) has been shown on the performance of a multi-relay system using opportunistic relay selection with outdated CSI. However, the analysis is limited to Rayleigh distributed channel model and average bit error rate expressions are derived for general order PSK, PAM and SQAM schemes only. This renders the work in [27] limited to singular fading, and recent power efficient modulation schemes have not been considered.

B. CONTRIBUTIONS

To the best of authors' knowledge, ASER analysis of various QAM schemes (HQAM, RQAM and XQAM) for a multi-relay system over a generalized fading channel (i.n.i.d. Nakagami-m fading) with imperfect CSI, and NLPA at the relays is not available in the literature. For the first time, in this work, an AF multi-relay system over i.n.i.d. Nakagami-m fading links with both integer and non-integer fading parameters is considered[2] where signals from the best relay, and source-to-destination ($S-D$) links are finally combined using MRC at the destination. Further, imperfect CSI, and NLPA at the relays are considered.

From this prospective, major contributions of this paper are:

- End-to-end instantaneous SNR of the considered AF multi-relay system is derived which comprises of the CEE due to the imperfect CSI, and NLD due to the presence of NLPA at the relays.
- Closed-form expressions for the lower-bound (LB) of the outage probability over i.n.i.d. Nakagami-m fading links with integer as well as non-integer valued fading parameters are derived and asymptotic analysis on the outage probability is performed in high SNR regime to obtain the diversity order of the considered system. Further, impact of the NLPA on the outage performance is observed by considering various threshold SNRs for the outage probability. Additionally, impact of the number of relays (N), and placement of the relays on the outage performance is also illustrated.
- Based on the CDF approach, closed-form LB expressions of the ASER for general order HQAM, general order RQAM and 32-XQAM schemes are derived. Further, a comparative analysis of ASER for various QAM schemes with different constellations is presented.
- Impact of fading parameter (m), number of relays (N), CEE and NLD is highlighted on the system performance and useful insights have been obtained.

Rest of the paper is organized as follows. In Section II, the considered system and channel models are presented. Section III consists of the outage probability analysis of the considered system. Asymptotic analysis on the outage probability is shown in Section IV. In Section V, ASER expressions for various QAM schemes with different constellation orders are derived. Theoretical and simulation results are presented in Section VI. Finally, conclusions are drawn in Section VII.

Notations: $Nak(m_i, \Omega_i)$ represents the Nakagami-m distribution with fading severity m_i and average power Ω_i. $x \sim \mathcal{CN}(0, \Omega_x)$ represents a complex Gaussian random variable with 0 mean and variance Ω_x. $F(\cdot), f(\cdot)$ and $u(\cdot)$, denote the cumulative distribution function (CDF), probability density function (PDF) and unit-step function of a random variable, respectively. $\mathcal{P}(\cdot)$, $\mathbb{E}[\cdot]$, $(\cdot)^*$, $\Gamma(\cdot)$, $\Gamma(\cdot,\cdot)$ and $\Upsilon(\cdot,\cdot)$ represent the probability, statistical expectation operator, complex conjugate, complete, upper incomplete, and lower incomplete gamma functions, respectively. $\mathrm{B}(\cdot,\cdot)$, ${}_1F_1(\cdot;\cdot;\cdot)$ and ${}_2F_1(\cdot,\cdot;\cdot;\cdot)$ represent the Beta function, confluent hypergeometric function of first kind and Gaussian hypergeometric function, respectively.

II. SYSTEM AND CHANNEL MODELS

In this work, a dual-hop AF multi-relay system with the best relay selection is considered. The end-to-end communication between the source S and the destination D is accomplished through a direct $S-D$ link, and through N indirect links using $R_1, R_2, \ldots, R_N$ relay nodes as shown in FIGURE 1. All the nodes are equipped with single antenna and communicate in half-duplex mode. Further, all the nodes are assumed synchronized at the symbol levels. Statistical behavior of the i^{th} link[3] is considered to be i.n.i.d. frequency flat complex Nakagami-m with uniform large scale path-loss. Amplitude of the i^{th} link's channel coefficient (h_i) is modeled

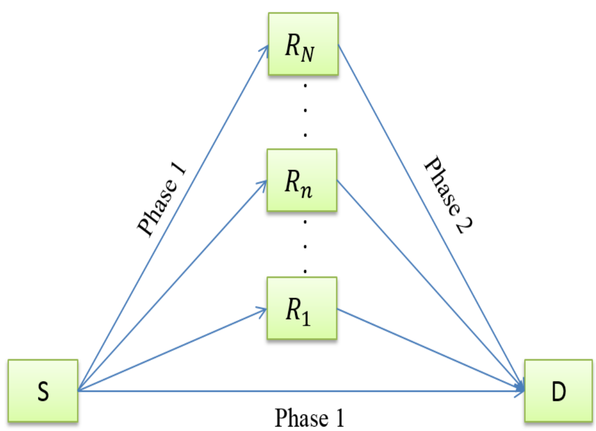

FIGURE 1. Dual-hop multi-relay AF system with best relay selection and NLPA at the relay.

[2]In the literature, most of the work is limited to integer value of fading parameter for the Nakagami-m distributed links. However, in practice, fading parameter m can take any arbitrary value. Thus, in this work, we focus on both integer and non-integer values of fading parameters for generality and completeness.

as $Nak(m_i, \Omega_i)$. Distance of the i^{th} link between the two nodes is represented by d_i. It is considered that all the relay nodes are placed in proximity, and hence, inter-relay distance is very small as compared to the distances of the relays from S and D.

CSI at the relay and destination nodes is assumed to be unknown and hence, minimum mean squared error (MMSE) estimation is performed at R_n and D. Let $\hat{h}_i$ be the estimate of h_i. Thus, according to MMSE, equality $h_i = (\hat{h}_i + e_i)$ holds between them where e_i is the CEE which can be modeled as $e_i \sim \mathcal{CN}(0, \Omega_{e_i})$. From the principal of orthogonality, estimation error for optimum MMSE is orthogonal to the channel realization h_i, i.e., $\mathbb{E}[e_i h_i^*] = 0$ which corresponds to $\Omega_{h_i} = \hat{\Omega}_{h_i} + \Omega_{e_i}$ [17]. The variance of CEE is considered as $\Omega_{e_i} = \frac{\Omega_{h_i}}{(1+\rho\gamma_0\Omega_{h_i})}$. Hence, $\hat{\Omega}_{h_i} = \frac{\rho\gamma_0\Omega_{h_i}^2}{(1+\rho\gamma_0\Omega_{h_i})}$, where $\gamma_0 = P_s/\Omega_0$ represents the average transmit SNR, and $\rho > 0$ represents the quality of channel estimation [18].

In the first transmission phase, S transmits information signal (X) with source power (P_s) to R_n and D, simultaneously. Thus, the respective signals received at the n^{th} relay and D will be

$$y_{sr_n} = \sqrt{P_s}(\hat{h}_{sr_n} + e_{sr_n})X + n_{sr_n}, \tag{1}$$
$$y_{sd} = \sqrt{P_s}(\hat{h}_{sd} + e_{sd})X + n_{sd}, \tag{2}$$

where $n_i \sim \mathcal{CN}(0, \Omega_0)$ is the AWGN associated with the i^{th} link with identical noise variance Ω_0. During the second phase of transmission, R_n amplifies the signal received from S with an amplification factor $G_n = \sqrt{\frac{P_r}{P_s(|\hat{h}_{sr_n}|^2+\Omega_{e_{sr_n}})+\Omega_0}}$. Thus, signal at n^{th} relay will be $y'_{R_n} = G_n y_{sr_n}$. Further, NLPA is considered at each of the relays which can be modeled as a memoryless function. According to the extension of the Bussgang's theorem, output of a memoryless non-linear system can be expressed as the summation of the attenuated replicas of the input signal with an uncorrelated noise signal [27]–[29]. Hence, output of the NLPA can be expressed as

$$y_{R_n} = K_0 y'_{R_n} + N_D, \tag{3}$$

where K_0 is constant and $N_D \sim \mathcal{CN}(0, \Omega_{N_D})$ is the NLD [22], [24], [26], [27], [30]. Closed-form expressions of K_0 and Ω_{N_D} are $K_0 = 1 - e^{-\left(\frac{A_{sat}^2}{P_r}\right)} + \frac{A_{sat}\sqrt{\pi}}{2\sqrt{P_r}}\mathrm{erfc}\left(\frac{A_{sat}}{\sqrt{P_r}}\right)$ and $\Omega_{N_D} = P_r(1 - e^{-\left(\frac{A_{sat}^2}{P_r}\right)} - |K_0|^2)$, respectively for the commonly used soft envelop limiter (SEL) PA model [22], [30]. Here A_{sat} represents the saturation amplitude of the PA and erfc$(\cdot)$ is the complementary error function.

Finally, output of the NLPA is forwarded to D. Thus, the signal received from the n^{th} relay to D can be expressed as

$$\begin{aligned} y_{r_nd} &= y_{R_n}(\hat{h}_{r_nd} + e_{r_nd}) + n_{r_nd} \\ &= G_nK_0\sqrt{P_s}(\hat{h}_{sr_n} + e_{sr_n})(\hat{h}_{r_nd} + e_{r_nd})X + n_{r_nd} \\ &\quad + G_nK_0(\hat{h}_{r_nd} + e_{r_nd})n_{sr_n} + (\hat{h}_{r_nd} + e_{r_nd})N_D. \end{aligned} \tag{4}$$

Thus, instantaneous end-to-end SNR of $S - R_n - D$ link can be written as (5), as shown at the bottom of this page, where $\hat{\gamma}_{sr_n} = \frac{P_s|\hat{h}_{sr_n}|^2}{\Omega_0}$ and $\hat{\gamma}_{r_nd} = \frac{P_rK_0^2|\hat{h}_{r_nd}|^2}{\Omega_0}$ represent the instantaneous estimated gains of $S-R_n$ and R_n-D links, respectively. Further, $\gamma_{pa} = \frac{P_rK_0^2}{\Omega_0}$ represents the instantaneous gain of the PA. Similarly, $L_{sr_n} = (1 + \varepsilon_{r_nd})$ and $L_{r_nd} = (1 + \varepsilon_{sr_n})$, where $\varepsilon_{sr_n} = \frac{P_s\Omega_{e_{sr_n}}}{\Omega_0}$ and $\varepsilon_{r_nd} = \frac{P_rK_0^2\Omega_{e_{r_nd}}}{\Omega_0}$.

For moderate and high SNRs, for mathematical tractability, term $(\gamma_{pa}L_{sr_n}L_{r_nd} + \hat{\gamma}_{r_nd}L_{r_nd} + \hat{\gamma}_{sr_n}\varepsilon_{r_nd} + L_{r_nd}\varepsilon_{r_nd})$ can be ignored from (5) by assuming that both the estimation errors and noise variances are small in practice [17], [18], [31]. Thus, for moderate and high SNRs, (5) can be approximated as

$$\gamma_{sr_nd} = \frac{\hat{\gamma}_{sr_n}\hat{\gamma}_{r_nd}\gamma_{pa}}{\hat{\gamma}_{sr_n}\gamma_{pa}L_{sr_n} + \gamma_{pa}\hat{\gamma}_{r_nd}L_{r_nd} + \hat{\gamma}_{sr_n}\hat{\gamma}_{r_nd}}. \tag{6}$$

To make the analysis mathematically tractable, γ_{sr_nd} can be further approximated with its lower-bound (LB) and upper-bound (UB) as

$$\gamma_{sr_nd}^{LB} \le \gamma_{sr_nd} \le \gamma_{sr_nd}^{UB}, \tag{7}$$

where

$$\gamma_{sr_nd}^{LB} = \frac{1}{3}\min\left(\frac{\hat{\gamma}_{sr_n}}{L_{r_nd}}, \gamma_{pa}, \frac{\hat{\gamma}_{r_nd}}{L_{sr_n}}\right), \tag{8}$$
$$\gamma_{sr_nd}^{UB} = \min\left(\frac{\hat{\gamma}_{sr_n}}{L_{r_nd}}, \gamma_{pa}, \frac{\hat{\gamma}_{r_nd}}{L_{sr_n}}\right). \tag{9}$$

Similarly, instantaneous SNR of $S - D$ link can be given as

$$\gamma_{sd} = \frac{\hat{\gamma}_{sd}}{L_{sd}}, \tag{10}$$

where $\hat{\gamma}_{sd} = \frac{P_s|\hat{H}_{sd}|^2}{\Omega_0}$, $L_{sd} = (1 + \varepsilon_{sd})$ and $\varepsilon_{sd} = \frac{P_s\Omega_{e_{sd}}}{\Omega_0}$.

Finally, the best relay is selected and MRC between n^{th} best relay and $S - D$ links is performed at the destination. Thus, end-to-end SNR at D can be given as

$$\gamma_{e2e} = \gamma_{sd} + \gamma_{sr_nd}^{*}. \tag{11}$$

where $\gamma_{sr_nd}^{*} = \underset{n\in\{1,\ldots,N\}}{\mathrm{argmax}}\{\gamma_{sr_nd}\}$.

[3]The $i \in (sd, sr_n, r_nd)$, where $1 \le n \le N$ denotes the indexing of relays.

$$\gamma_{sr_nd} = \frac{\hat{\gamma}_{sr_n}\hat{\gamma}_{r_nd}\gamma_{pa}}{\hat{\gamma}_{sr_n}\gamma_{pa}L_{sr_n} + \gamma_{pa}\hat{\gamma}_{r_nd}L_{r_nd} + \hat{\gamma}_{sr_n}\hat{\gamma}_{r_nd} + \gamma_{pa}L_{sr_n}L_{r_nd} + \hat{\gamma}_{r_nd}L_{r_nd} + \hat{\gamma}_{sr_n}\varepsilon_{r_nd} + L_{r_nd}\varepsilon_{r_nd}}. \tag{5}$$

III. OUTAGE PROBABILITY

Outage probability is one of the important performance measures which is mainly used in slow fading scenario. Outage probability is defined as the probability that the end-to-end SNR of the considered system reaches below a predefined threshold (γ_{th}). LB of the outage probability (for the considered UB of the end-to-end SNR (γ_{e2e}^{UB})) can be given as

$$\begin{aligned}\mathcal{P}_{out}^{LB}(\gamma_{th}) &= \mathcal{P}(\gamma_{e2e}^{UB} \leq \gamma_{th}) \\ &= \mathcal{P}((\gamma_{sd} + \underset{n\in\{1,\ldots,N\}}{\operatorname{argmax}}\{\gamma_{sr_nd}^{UB}\}) \leq \gamma_{th}) \\ &= \int_0^\infty f_{\gamma_{sd}}(x) F_{\gamma_{sr_nd}^*}(\gamma_{th} - x)dx, \end{aligned} \tag{12}$$

where $f_{\gamma_{sd}}(\cdot)$ and $F_{\gamma_{sr_nd}^*}(\cdot)$ represent the PDF of direct $S-D$ link and the CDF of the best indirect $S - R_n - D$ link, respectively.

Theorem 1: Depending upon the value of fading parameter, outage analysis is categorized into two following cases:

A. INTEGER VALUED FADING PARAMETER

For integer valued fading parameter, closed-form expression for the LB of the outage probability can be expressed as

$$\begin{aligned}\mathcal{P}_{out}^{LB}(\gamma_{th}) &= \frac{1}{\Gamma(m_{sd})}\Upsilon(m_{sd}, C_3\gamma_{th}) + \Psi_1\gamma_{th}^{(j+k-l)} \\ &\quad \times e^{-C_2\gamma_{th}}\Big[\Gamma\Big(m_{sd}+l, \gamma_{\max}(C_3 - C_2)\Big) \\ &\quad - \Gamma\Big(m_{sd}+l, \gamma_{th}(C_3 - C_2)\Big)\Big], \end{aligned} \tag{13}$$

where $\Psi_1 = \sum_{n=1}^{N}\sum_{j=0}^{n(m_{sr_n}-1)}\sum_{k=0}^{n(m_{r_nd}-1)}\binom{N}{n}(-1)^n\varphi_j^n\varphi_k^n \times \frac{C_3^{m_{sd}}}{\Gamma(m_{sd})}\eta_1^j\eta_2^k\sum_{l=0}^{j+k}\binom{j+k}{l}(-1)^l(C_3 - C_2)^{-(m_{sd}+l)}$, $C_2 = n(\eta_1 + \eta_2)$, $C_3 = \frac{m_{sd}(1+\varepsilon_{sd})}{\hat{\bar{\gamma}}_{sd}}$, $\eta_1 = \left(\frac{m_{sr_n}L_{r_nd}}{\hat{\bar{\gamma}}_{sr_n}}\right)$, $\eta_2 = \left(\frac{m_{r_nd}L_{sr_n}}{\hat{\bar{\gamma}}_{r_nd}}\right)$ and $\gamma_{\max} = \max(0, \gamma_{th} - \bar{\gamma}_{pa})$.

B. NON-INTEGER VALUED FADING PARAMETER

For the non-integer valued fading parameter, closed-form expression for the LB of the outage probability can be expressed as

$$\begin{aligned}\mathcal{P}_{out}^{LB}(\gamma_{th}) &= \sum_{g=0}^{\infty}\frac{C_3^{m_{sd}+g}}{\Gamma(m_{sd}+g+1)}e^{-C_3\gamma_{th}}\gamma_{th}^{m_{sd}+g} + \Psi_2\gamma_{th}^{(C_5-i_1)} \\ &\quad \times e^{-C_4\gamma_{th}}\Big[\Gamma(m_{sd}+i_1, (C_3 - C_4)\gamma_{max}) \\ &\quad - \Gamma(m_{sd}+i_1, (C_3 - C_4)\gamma_{th})\Big], \end{aligned} \tag{14}$$

where $\Psi_2 = \frac{C_3^{m_{sd}}}{\Gamma(m_{sd})}\sum_{n=1}^{N}\binom{N}{n}\sum_{p=0}^{n}\binom{n}{p}\sum_{p_1=0}^{n}\binom{n}{p_1}(-1)^{(n+p+p_1)}\sum_{\upsilon_1=0}^{\infty}\sum_{\upsilon_2=0}^{\infty}\psi_{\upsilon_1}^{p}\psi_{\upsilon_2}^{p_1}\sum_{i_1=0}^{\infty}(-1)^{i_1}\binom{C_5}{i_1}(C_3 - C_4)^{-(m_{sd}+i_1)}$, $C_4 = (p\eta_1 + p_1\eta_2)$ and $C_5 = (\upsilon_1 + \upsilon_2 + pm_{sr_n} + p_1m_{r_nd})$.

Proof: See Appendix A.

IV. ASYMPTOTIC OUTAGE PROBABILITY

In this Section, asymptotic analysis on the outage probability is performed to obtain the diversity order of the considered multi-relay system.

Theorem 2: As the outage probability consists of the term $\gamma_{max} = \max(0, \gamma_{th} - \bar{\gamma}_{pa})$, asymptotic analysis on the outage probability is performed for two cases when $\gamma_{th} < \bar{\gamma}_{pa}$, and when $\gamma_{th} > \bar{\gamma}_{pa}$ to illustrate the impact of NLD caused by the NLPA on the system performance.

Case 1: For $\gamma_{th} < \bar{\gamma}_{pa}$

For the considered case, closed-form asymptotic outage probability expression for the arbitrary value of fading parameter can be given as

$$\begin{aligned}\mathcal{P}_{out}^{asym}(\gamma_{th}) &\approx \sum_{n=0}^{N}\sum_{j=0}^{n}\sum_{k=0}^{n}\binom{N}{n}\binom{n}{j}\binom{n}{k}(-1)^{n+j+k} \\ &\quad \times \mathrm{B}(jm_{sr_n} + km_{r_nd} + 1, m_{sd}) \\ &\quad \times \frac{(C_3\gamma_{th})^{m_{sd}}}{\Gamma(m_{sd})}\frac{(\eta_1\gamma_{th})^{jm_{sr_n}}}{(m_{sr_n}!)^j}\frac{(\eta_2\gamma_{th})^{km_{r_nd}}}{(m_{r_nd}!)^k}. \end{aligned} \tag{15}$$

In (15), asymptotic outage probability is derived for $\gamma_{th} < \bar{\gamma}_{pa}$ which depends upon N, m_{sd}, m_{sr_n}, m_{r_nd}, C_3, η_1 and η_2. Further, C_3, η_1 and η_2 depend on CEE coefficients L_{sd}, L_{sr_n} and L_{r_nd}, respectively. For perfect CSI case, there is no CEE and hence, $L_i = 1$ as $\varepsilon_i = 0$ due to $\Omega_{e_i} = 0$. Therefore, from (15) we can conclude that the diversity order of the considered system for $\gamma_{th} < \bar{\gamma}_{pa}$ is $[m_{sd} + N\min(m_{sr_n}, m_{r_nd})]$ with perfect CSI consideration depends on N, m_{sd}, m_{sr_n} and m_{r_nd}.

For imperfect CSI, $\left(\Omega_{e_i} = \frac{\Omega_{h_i}}{(1+\rho\gamma_0\Omega_{h_i})}\right) \rightarrow 0$ for high transmit SNR ($\gamma_0 \rightarrow \infty$). Thus, the diversity order remains same as in perfect CSI case, since the variance of CEE is dependent on the SNR. However, degradation in the outage performance is observed.

Case 2: For $\gamma_{th} > \bar{\gamma}_{pa}$

For the considered case, closed-form expression for the asymptotic outage probability for arbitrary value of fading parameter can be given as

$$\mathcal{P}_{out}^{asym}(\gamma_{th}) \approx \frac{C_3^{m_{sd}}}{m_{sd}!}\left(1 - \frac{\bar{\gamma}_{pa}}{\gamma_{th}}\right)^{m_{sd}}. \tag{16}$$

From (16), it is clear that the asymptotic outage probability consists of m_{sd} and C_3. Thus, considering perfect CSI, from (16) it is concluded that the diversity order of the considered system is m_{sd} and is independent of N, m_{sr_n} and m_{r_nd}. For imperfect CSI, $\Omega_{e_i} \rightarrow 0$ as $\gamma_0 \rightarrow \infty$. Hence, the same diversity order is achieved with some degradation in the outage performance.

Proof: See Appendix B.

V. ASER ANALYSIS

A CDF based generalized ASER expression for digital modulation technique is given as

$$\mathcal{P}_s(e) = -\int_0^\infty \mathcal{P}_s'(e|\gamma)\mathcal{P}_{out}(\gamma)d\gamma, \tag{17}$$

where $\mathcal{P}_s'(e|\gamma)$ represents the first derivative of the conditional SEP $\big(\mathcal{P}_s(e|\gamma)\big)$ for the received SNR. To make the ASER analysis mathematically tractable, LB of the outage probability ($\mathcal{P}_{out}^{LB}(\gamma)$) is considered. Thus, the LB expressions for the ASER for various QAM schemes are shown below:

A. HEXAGONAL QAM

Theorem 3:

1) INTEGER VALUED FADING PARAMETER

For integer valued fading parameter, analytical ASER expression for the general order HQAM scheme can be given as

$$
\begin{aligned}
\mathcal{P}_e^H &= -\frac{1}{2}\sqrt{\frac{\alpha}{2\pi}}(\tau_c-\tau)\Big[\mathbb{F}\Big(\frac{1}{2},\frac{\alpha}{2}\Big)+\Psi_1\Big\{\mathbb{G}\Big(\frac{1}{2},\frac{\alpha}{2}\Big)\\
&\quad+\Xi\mathbb{H}\Big(\frac{1}{2},\frac{\alpha}{2}\Big)-\mathbb{I}\Big(\frac{1}{2},\frac{\alpha}{2}\Big)\Big\}\Big]+\frac{\tau_c}{3}\sqrt{\frac{\alpha}{3\pi}}\Big[\mathbb{F}\Big(\frac{1}{2},\frac{\alpha}{3}\Big)\\
&\quad+\Psi_1\Big\{\mathbb{G}\Big(\frac{1}{2},\frac{\alpha}{3}\Big)+\Xi\mathbb{H}\Big(\frac{1}{2},\frac{\alpha}{3}\Big)-\mathbb{I}\Big(\frac{1}{2},\frac{\alpha}{3}\Big)\Big\}\Big]-\frac{\tau_c}{2}\sqrt{\frac{\alpha}{6\pi}}\\
&\quad\times\Big[\mathbb{F}\Big(\frac{1}{2},\frac{\alpha}{6}\Big)+\Psi_1\Big\{\mathbb{G}\Big(\frac{1}{2},\frac{\alpha}{6}\Big)+\Xi\mathbb{H}\Big(\frac{1}{2},\frac{\alpha}{6}\Big)-\mathbb{I}\Big(\frac{1}{2},\frac{\alpha}{6}\Big)\Big\}\Big]\\
&\quad-\sum_{r=0}^{\infty}\frac{(1)_r}{r!(1.5)_r}\Big[\frac{2\tau_c\alpha}{9\pi}\Big(\frac{\alpha}{3}\Big)^r-\Big(\frac{\tau_c\alpha}{2\sqrt{3}\pi}\Big(\Big(\frac{\alpha}{2}\Big)^r\\
&\quad+\Big(\frac{\alpha}{6}\Big)^r\Big)\Big)\Big]\Big[\mathbb{F}\Big(r+1,\frac{2\alpha}{3}\Big)+\Psi_1\Big\{\mathbb{G}\Big(r+1,\frac{2\alpha}{3}\Big)\\
&\quad+\Xi\mathbb{H}\Big(r+1,\frac{2\alpha}{3}\Big)-\mathbb{I}\Big(r+1,\frac{2\alpha}{3}\Big)\Big\}\Big],
\end{aligned}
\tag{18}
$$

where $\Xi = e^{\gamma_{pa}(C_3-C_2)}\sum_{l_1=0}^{m_{sd}+l-1}\frac{(C_3-C_2)^{l_1}}{l_1!}\sum_{u=0}^{l_1}\binom{l_1}{u}(-\gamma_{pa})^{(l_1-u)}$, $\mathbb{F}(\theta,\phi)=\frac{C_3^{m_{sd}}\Gamma(m_{sd}+\theta)}{m_{sd}!(C_3+\phi)^{(m_{sd}+\theta)}}\,{}_2F_1\Big(1,m_{sd}+\theta;m_{sd}+1;\frac{C_3}{C_3+\phi}\Big)$, $\mathbb{G}(\theta,\phi)=\Gamma(m_{sd}+l)(C_2+\phi)^{-(j+k-l+\theta)}\Upsilon(j+k-l+\theta,(C_2+\phi)\gamma_{pa})$, $\mathbb{H}(\theta,\phi)=\Gamma(m_{sd}+l)(C_3+\phi)^{-(j+k+u-l+\theta)}\Gamma(j+k+u-l+\theta,(C_3+\phi)\gamma_{pa})$, and $\mathbb{I}(\theta,\phi)=\frac{(C_3-C_2)^{m_{sd}+l}\Gamma(m_{sd}+j+k+\theta)}{(j+k-l+\theta)(C_3+\phi)^{(m_{sd}+j+k+\theta)}}\,{}_2F_1\Big(1,m_{sd}+j+k+\theta;j+k-l+\theta+1;\frac{C_2+\phi}{C_3+\phi}\Big)$. Further, α, τ and τ_c are constants defined in [13], [32] and their different values are used to select various HQAM constellations.

2) NON-INTEGER VALUED FADING PARAMETER

For non-integer valued fading parameter, ASER expression for the general order HQAM scheme can be given as

$$
\begin{aligned}
\mathcal{P}_e^H &= \frac{1}{2}\sqrt{\frac{\alpha}{2\pi}}(\tau_c-\tau)\Big[-C_6\mathbb{I}_1\Big(\frac{1}{2},\frac{\alpha}{2}\Big)+\Psi_2\Big\{\mathbb{I}_2\Big(\frac{1}{2},\frac{\alpha}{2}\Big)\\
&\quad-\Gamma(m_{sd}+i_1)\mathbb{I}_3\Big(\frac{1}{2},\frac{\alpha}{2}\Big)+\Psi_3\mathbb{I}_4\Big(\frac{1}{2},\frac{\alpha}{2}\Big)\Big\}\Big]\\
&\quad-\frac{K_c}{3}\sqrt{\frac{\alpha}{3\pi}}\Big[-C_6\mathbb{I}_1\Big(\frac{1}{2},\frac{\alpha}{3}\Big)+\Psi_2\Big\{\mathbb{I}_2\Big(\frac{1}{2},\frac{\alpha}{3}\Big)\\
&\quad-\Gamma(m_{sd}+i_1)\mathbb{I}_3\Big(\frac{1}{2},\frac{\alpha}{3}\Big)+\Psi_3\mathbb{I}_4\Big(\frac{1}{2},\frac{\alpha}{3}\Big)\Big\}\Big]\\
&\quad+\frac{K_c}{2}\sqrt{\frac{\alpha}{6\pi}}\Big[-C_6\mathbb{I}_1\Big(\frac{1}{2},\frac{\alpha}{6}\Big)+\Psi_2\Big\{\mathbb{I}_2\Big(\frac{1}{2},\frac{\alpha}{6}\Big)\\
&\quad-\Gamma(m_{sd}+i_1)\mathbb{I}_3\Big(\frac{1}{2},\frac{\alpha}{6}\Big)+\Psi_3\mathbb{I}_4\Big(\frac{1}{2},\frac{\alpha}{6}\Big)\Big\}\Big]\\
&\quad+\sum_{r=0}^{\infty}\frac{(1)_r}{r!(1.5)_r}\Big[\frac{2\tau_c\alpha}{9\pi}\Big(\frac{\alpha}{3}\Big)^r-\Big(\frac{\tau_c\alpha}{2\sqrt{3}\pi}\Big(\Big(\frac{\alpha}{2}\Big)^r\\
&\quad+\Big(\frac{\alpha}{6}\Big)^r\Big)\Big)\Big]\Big[-C_6\mathbb{I}_1\Big(r+1,\frac{2\alpha}{3}\Big)+\Psi_2\Big\{\mathbb{I}_2\Big(r+1,\frac{2\alpha}{3}\Big)\\
&\quad-\Gamma(m_{sd}+i_1)\mathbb{I}_3\Big(r+1,\frac{2\alpha}{3}\Big)+\Psi_3\mathbb{I}_4\Big(r+1,\frac{2\alpha}{3}\Big)\Big\}\Big],
\end{aligned}
\tag{19}
$$

where $C_6=\sum_{g=0}^{\infty}\frac{C_3^{m_{sd}+g}}{\Gamma(m_{sd}+g+1)}$, $\Psi_3=\Gamma(m_{sd}+i_1)\sum_{g=0}^{\infty}\frac{1}{\Gamma(m_{sd}+i_1+g+1)}e^{(C_3-C_4)\gamma_{pa}}(C_3-C_4)^{(m_{sd}+i_1+g)}\sum_{q_1=0}^{\infty}\binom{m_{sd}+i_1+g}{q_1}(-\gamma_{pa})^{q_1}$, $\mathbb{I}_1(\theta,\phi)=\Gamma(m_{sd}+g+\theta)(\phi+C_3)^{-(m_{sd}+g+\theta)}$, $\mathbb{I}_2(\theta,\phi)=\frac{(C_3-C_4)^{(m_{sd}+i_1)}\Gamma(C_5+\theta+m_{sd})}{\Gamma(C_5-i_1+\theta)(C_3+\phi)^{(C_5+\theta+m_{sd})}}\,{}_2F_1\Big(1,(C_5+\theta+m_{sd});(C_5-i_1+\theta+1);\frac{C_4+\phi}{C_3+\phi}\Big)$, $\mathbb{I}_3(\theta,\phi)=\Gamma(C_5-i_1+\theta)(C_4+\phi)^{-(C_5-i_1+\theta)}$ and $\mathbb{I}_4(\theta,\phi)=\Gamma((C_5+m_{sd}+g-q_1+\theta),(C_3+\phi)\gamma_{pa})(C_3+\phi)^{-(C_5+m_{sd}+g-q_1+\theta)}$.

Proof: See Appendix C.

B. RECTANGULAR QAM

Theorem 4:

1) INTEGER VALUED FADING PARAMETER

For integer valued fading parameter, ASER expression for the general order RQAM scheme can be given as

$$
\begin{aligned}
\mathcal{P}_e^R &= \frac{a_0p_0(1-q_0)}{\sqrt{2\pi}}\Big[\mathbb{F}\Big(\frac{1}{2},\frac{a_0^2}{2}\Big)+\Psi_1\Big\{\mathbb{G}\Big(\frac{1}{2},\frac{a_0^2}{2}\Big)\\
&\quad+\Xi\mathbb{H}\Big(\frac{1}{2},\frac{a_0^2}{2}\Big)-\mathbb{I}\Big(\frac{1}{2},\frac{a_0^2}{2}\Big)\Big\}\Big]+\frac{b_0q_0(1-p_0)}{\sqrt{2\pi}}\\
&\quad\times\Big[\mathbb{F}\Big(\frac{1}{2},\frac{b_0^2}{2}\Big)+\Psi_1\Big\{\mathbb{G}\Big(\frac{1}{2},\frac{b_0^2}{2}\Big)+\Xi\mathbb{H}\Big(\frac{1}{2},\frac{b_0^2}{2}\Big)\\
&\quad-\mathbb{I}\Big(\frac{1}{2},\frac{b_0^2}{2}\Big)\Big\}\Big]+\sum_{r=0}^{\infty}\frac{(1)_r}{r!(1.5)_r}\frac{a_0b_0p_0q_0}{\pi}\Big[\Big(\frac{a_0^2}{2}\Big)^r\\
&\quad+\Big(\frac{b_0^2}{2}\Big)^r\Big]\Big[\mathbb{F}\Big(r+1,\frac{a_0^2+b_0^2}{2}\Big)\\
&\quad+\Psi_1\Big\{\mathbb{G}\Big(r+1,\frac{a_0^2+b_0^2}{2}\Big)+\Xi\mathbb{H}\Big(r+1,\frac{a_0^2+b_0^2}{2}\Big)\\
&\quad-\mathbb{I}\Big(r+1,\frac{a_0^2+b_0^2}{2}\Big)\Big\}\Big],
\end{aligned}
\tag{20}
$$

where $p_0=1-(1/M_I)$, $q_0=1-(1/M_Q)$, $a_0=\sqrt{6/((M_I^2-1)+(M_Q^2-1)\lambda^2)}$, $b_0=\lambda a_0$, and $\lambda=d_Q/d_I$ represents the ratio of quadrature and in-phase decision distances. Also, M_I and M_Q represent respectively the in-phase and quadrature phase constellation points.

2) NON-INTEGER VALUED FADING PARAMETER

For non-integer valued fading parameter, ASER expression for the general order RQAM scheme can be given as

$$\begin{aligned}\mathcal{P}_e^R &= \frac{a_0p_0(q_0-1)}{\sqrt{2\pi}}\Big[-C_6\mathbb{I}_1\Big(\frac{1}{2},\frac{a_0^2}{2}\Big)+\Psi_2\Big\{\mathbb{I}_2\Big(\frac{1}{2},\frac{a_0^2}{2}\Big)\\&\quad -\Gamma(m_{sd}+i_1)\mathbb{I}_3\Big(\frac{1}{2},\frac{a_0^2}{2}\Big)+\Psi_3\mathbb{I}_4\Big(\frac{1}{2},\frac{a_0^2}{2}\Big)\Big\}\Big]\\&\quad +\frac{b_0q_0(p_0-1)}{\sqrt{2\pi}}\Big[-C_6\mathbb{I}_1\Big(\frac{1}{2},\frac{b_0^2}{2}\Big)+\Psi_2\Big\{\mathbb{I}_2\Big(\frac{1}{2},\frac{b_0^2}{2}\Big)\\&\quad -\Gamma(m_{sd}+i_1)\mathbb{I}_3\Big(\frac{1}{2},\frac{b_0^2}{2}\Big)+\Psi_3\mathbb{I}_4\Big(\frac{1}{2},\frac{b_0^2}{2}\Big)\Big\}\Big]\\&\quad -\sum_{r=0}^{\infty}\frac{(1)_r}{r!(1.5)_r}\frac{a_0b_0p_0q_0}{\pi}\Big[\Big(\frac{a_0^2}{2}\Big)^r+\Big(\frac{b_0^2}{2}\Big)^r\Big]\\&\quad \times\Big[-6\mathbb{I}_1\Big(r+1,\frac{a_0^2+b_0^2}{2}\Big)+\Psi_2\Big\{\mathbb{I}_2\Big(r+1,\frac{a_0^2+b_0^2}{2}\Big)\\&\quad -\Gamma(m_{sd}+i_1)\mathbb{I}_3\Big(r+1,\frac{a_0^2+b_0^2}{2}\Big)\\&\quad +\Psi_3\mathbb{I}_4\Big(r+1,\frac{a_0^2+b_0^2}{2}\Big)\Big\}\Big]. \qquad (21)\end{aligned}$$

Proof: See Appendix D.

C. CROSS QAM

Theorem 5:

1) INTEGER VALUED FADING PARAMETER

For integer valued fading parameter, ASER expression for 32-XQAM scheme can be given as

$$\begin{aligned}\mathcal{P}_e^X &= \frac{1}{8}\Big[\frac{3}{2}\sqrt{\frac{\chi}{\pi}}\Big[\mathbb{F}\Big(\frac{1}{2},\chi\Big)+\Psi_1\Big\{\mathbb{G}\Big(\frac{1}{2},\chi\Big)+\Xi\mathbb{H}\Big(\frac{1}{2},\chi\Big)\\&\quad -\mathbb{I}\Big(\frac{1}{2},\chi\Big)\Big\}\Big]+\sqrt{\frac{\chi}{2\pi}}\Big[\mathbb{F}\Big(\frac{1}{2},2\chi\Big)+\Psi_1\Big\{\mathbb{G}\Big(\frac{1}{2},2\chi\Big)\\&\quad +\Xi\mathbb{H}\Big(\frac{1}{2},2\chi\Big)-\mathbb{I}\Big(\frac{1}{2},2\chi\Big)\Big\}\Big]+\frac{23\chi}{\pi}\sum_{r=0}^{\infty}\frac{(1)_r}{r!(1.5)_r}\chi^r\\&\quad \times\Big[\mathbb{F}(r+1,2\chi)+\Psi_1\{\mathbb{G}(r+1,2\chi)\\&\quad +\Xi\mathbb{H}(r+1,2\chi)-\mathbb{I}(r+1,2\chi)\}\Big]\Big], \qquad (22)\end{aligned}$$

where $\chi = 48/(31M-32)$.

2) NON-INTEGER VALUED FADING PARAMETER

For non-integer valued fading parameter, ASER expression for 32-XQAM scheme can be given as

$$\begin{aligned}\mathcal{P}_e^X &= -\frac{1}{8}\Big[\frac{3}{2}\sqrt{\frac{\chi}{\pi}}\Big[-C_6\mathbb{I}_1\Big(\frac{1}{2},\chi\Big)+\Psi_2\Big\{\mathbb{I}_2\Big(\frac{1}{2},\chi\Big)\\&\quad -\Gamma(m_{sd}+i_1)\mathbb{I}_3\Big(\frac{1}{2},\chi\Big)+\Psi_3\mathbb{I}_4\Big(\frac{1}{2},\chi\Big)\Big\}\Big]+\sqrt{\frac{\chi}{2\pi}}\\&\quad \times\Big[-C_6\mathbb{I}_1\Big(\frac{1}{2},2\chi\Big)+\Psi_2\Big\{\mathbb{I}_2\Big(\frac{1}{2},2\chi\Big)-\Gamma(m_{sd}+i_1)\\&\quad \times\mathbb{I}_3\Big(\frac{1}{2},2\chi\Big)+\Psi_3\mathbb{I}_4\Big(\frac{1}{2},2\chi\Big)\Big\}\Big]+\frac{23\chi}{\pi}\sum_{r=0}^{\infty}\frac{(1)_r}{r!(1.5)_r}\\&\quad \times\chi^r\Big[-C_6\mathbb{I}_1\Big(r+1,2\chi\Big)+\Psi_2\Big\{\mathbb{I}_2\Big(r+1,2\chi\Big)\\&\quad -\Gamma(m_{sd}+i_1)\mathbb{I}_3\Big(r+1,2\chi\Big)+\Psi_3\mathbb{I}_4\Big(r+1,2\chi\Big)\Big\}\Big]\Big]. \qquad (23)\end{aligned}$$

Proof: See Appendix E.

VI. THEORETICAL AND SIMULATION RESULTS

In this Section, theoretical and simulation results of the outage probability, asymptotic outage probability and ASER for the HQAM, RQAM and XQAM schemes are presented to demonstrate the performance of the considered multi-relay system. For analysis, $P_s = P_r = 0.5$ is used. Further, $\Omega_i = 1/d_i^a$ where a linear network geometry $d_{sr} + d_{rd} = 1$ with $d_{sr}, d_{rd} \in (0, 1)$ and path-loss factor $a = 4$ is considered. A SEL power amplifier model with saturation amplitude $A_{sat} = 1$ is considered at each of the relays whose average SNR is $\bar{\gamma}_{pa} = 17.5$ dB for $P_s = P_r = 0.5$. Various infinite series present in the analytical lower-bound outage probability expression (14), which also reflect in the ASER expressions of HQAM, RQAM and XQAM schemes for the non-integer fading parameter consideration. However, to obtain numerical values for the derived expressions, these infinite series must be truncated to some finite values. Truncation is performed in such a manner that reduces computational complexity with considerable accuracy. Thus, infinite summations g, i_1, υ_1 and υ_2 are truncated to fixed finite values G_1, I_1, V_1 and V_2, respectively, and $G_1 = 50$, $I_1 = 30$ and $V_1 = V_2 = 10$ are considered for considerable accuracy with acceptable computational complexity.

In FIGURE 2, theoretical, simulation and asymptotic outage probability against transmit SNR are compared for various threshold SNRs (10 dB, 20 dB). For comparison, various values of m_i, N, and NLPA at the relays are considered for perfect CSI ($\rho = \infty$), and imperfect CSI ($\rho = 1$) cases. For all the considered cases, simulation results match the theoretical results which validates the derived theoretical outage probability. Further, the theoretical results are always below the simulation results which justifies the LB of the outage probability. To obtain diversity order of the considered system, asymptotic analysis on the outage probability is also performed for $\gamma_{th} < \bar{\gamma}_{pa}$ and for $\gamma_{th} > \bar{\gamma}_{pa}$ cases. Considering perfect CSI, from the analysis it is observed that for $\gamma_{th} < \bar{\gamma}_{pa}$, diversity order is $[m_{sd} + N \min(m_{sr_n}, m_{r_nd})]$ which depends on m_{sd}, m_{sr_n}, m_{r_nd} and N. For $\gamma_{th} > \bar{\gamma}_{pa}$, diversity order of the considered network is m_{sd} which depends only on m_{sd} and hence, there is no impact of m_{sr_n}, m_{r_nd} and N on the outage performance. Further, for imperfect CSI ($\rho = 1$), diversity order remains same as in perfect CSI condition for both the cases (i.e. for $\gamma_{th} < \bar{\gamma}_{pa}$ and $\gamma_{th} > \bar{\gamma}_{pa}$) (since variance of CEE depends on SNR). However, degradation in outage performance is observed for all the considered cases with imperfect CSI as also reported in [7]. From FIGURE 2,

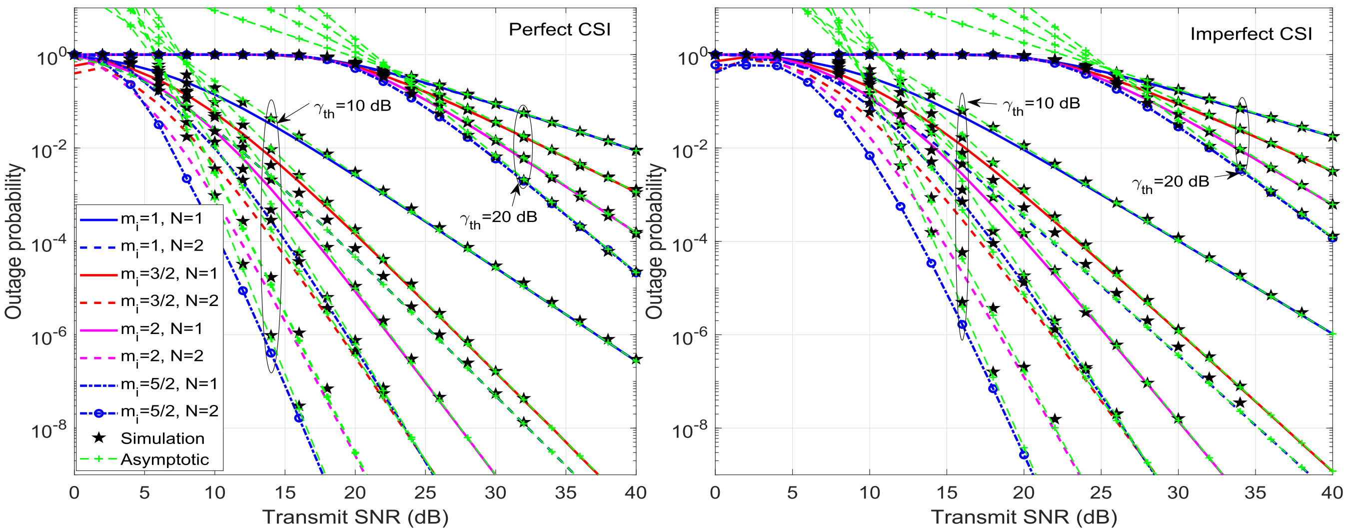

FIGURE 2. Comparison of theoretical, simulation and asymptotic results of outage probability with perfect and imperfect CSI, and NLPA at the relays.

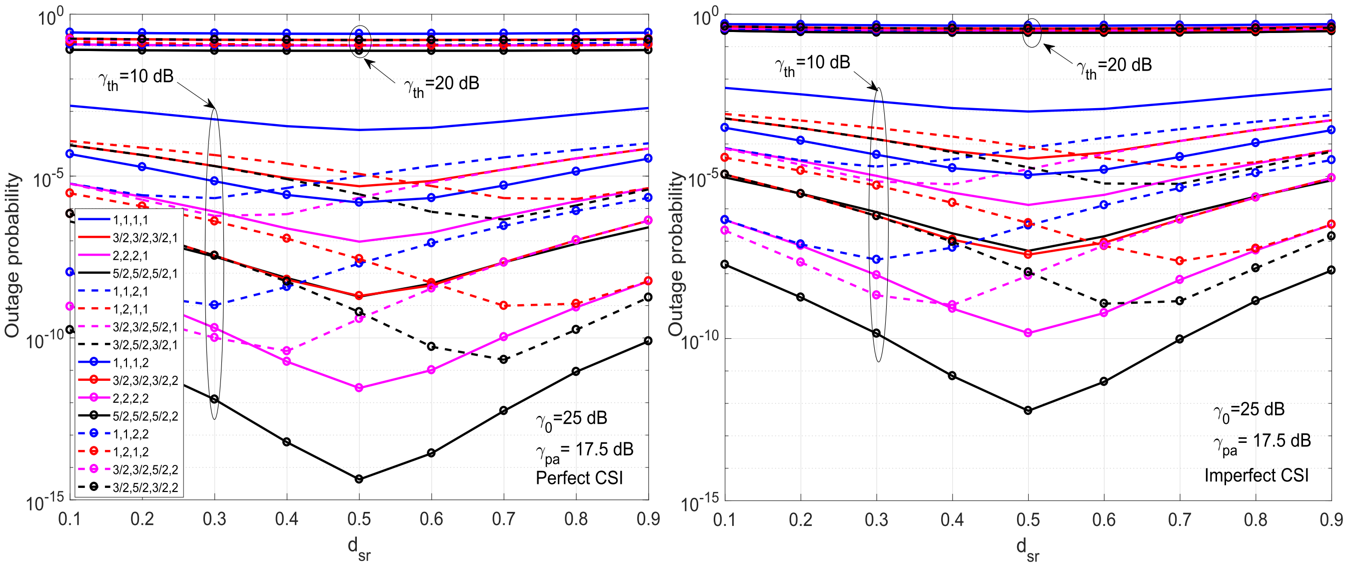

FIGURE 3. Comparative analysis of outage probability against normalized relay distance d_{sr} with perfect CSI (left) and imperfect CSI (right) cases, in the presence of NLPA at the relays.

it is observed that to obtain an outage probability of 10^{-4} for $\gamma_{th} < \bar{\gamma}_{pa}$ ($\gamma_{th} = 10$ dB) and for $m_i = 1$, around 8 dB SNR gain is achieved with the increase in N from 1 to 2. For $N = 1$, around 6.7 dB and 10 dB SNR gains are achieved with the increase in m_i from 1 to 3/2 and 1 to 2, respectively for perfect as well as imperfect CSI cases. Further, to achieve 10^{-4} outage probability, approx. 3 dB degradation in SNR is observed for imperfect CSI ($\rho = 1$) over perfect CSI case for all the combinations of m_i and N. For $\gamma_{th} > \bar{\gamma}_{pa}$ ($\gamma_{th} = 20$ dB), there is no impact of relay selection, and outage performance improves only with the increase in m_{sd}. Thus, it can be concluded that the improvement in the outage performance is more with the increase in m_i than N specially in the presence of NLPA at the relays.

In FIGURE 3, comparative analysis of theoretical results for the outage probability against normalized relay distance d_{sr} is illustrated for perfect CSI (left) as well as imperfect CSI (right) cases. For analysis, various combinations of m_{sr_n}, m_{r_nd} and m_{sd}, and different values of N with NLPA at the relays are considered. From analysis, it is observed that for $\gamma_{th} < \bar{\gamma}_{pa}$ and for $m_{sr_n} = m_{r_nd}$ (integer as well as non-integer values), optimum relay placement must be in the middle of S and D, irrespective of the values of m_{sd}. However, for unequal values of m_{sr_n} and m_{r_nd}, relay should be placed closer to S or D for higher value of m_{r_nd} or m_{sr_n}, respectively. Moreover, for $\gamma_{th} > \bar{\gamma}_{pa}$, diversity order of the considered network is m_{sd}. Thus, the outage performance is affected by only m_{sd} and there is no impact of the relay selection and the relay placement.

In FIGURE 4 and FIGURE 5, comparison of theoretical and simulation results of ASER for the 16-HQAM with perfect CSI and imperfect CSI, respectively are illustrated

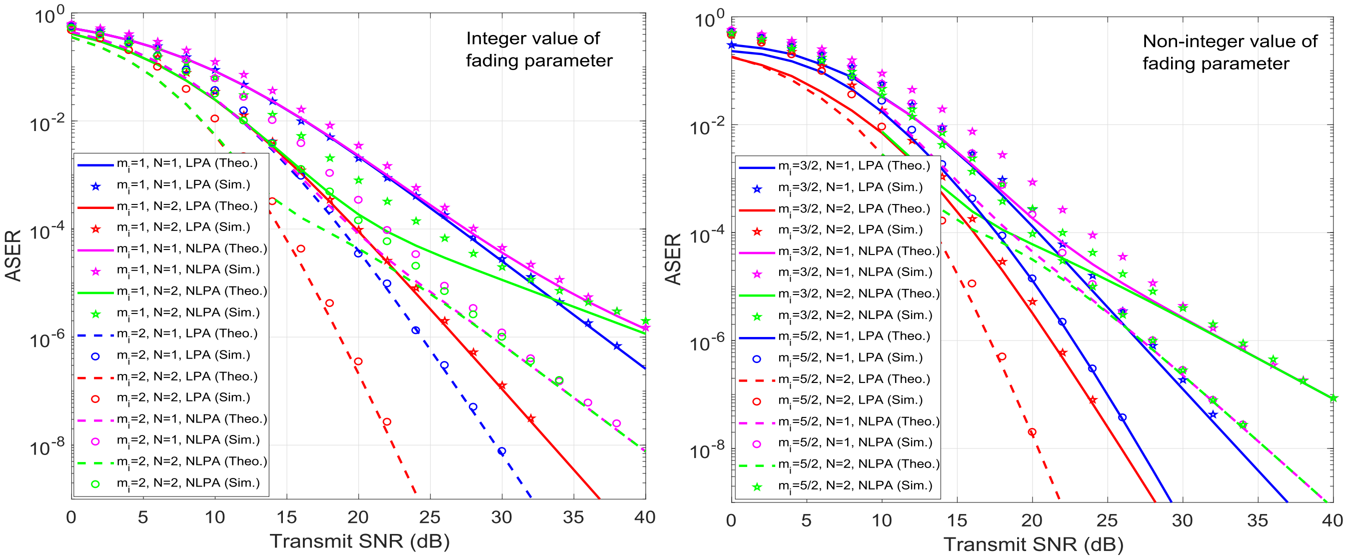

FIGURE 4. Comparison of theoretical and simulation results of ASER for 16-HQAM with perfect CSI, and NLPA at the relays.

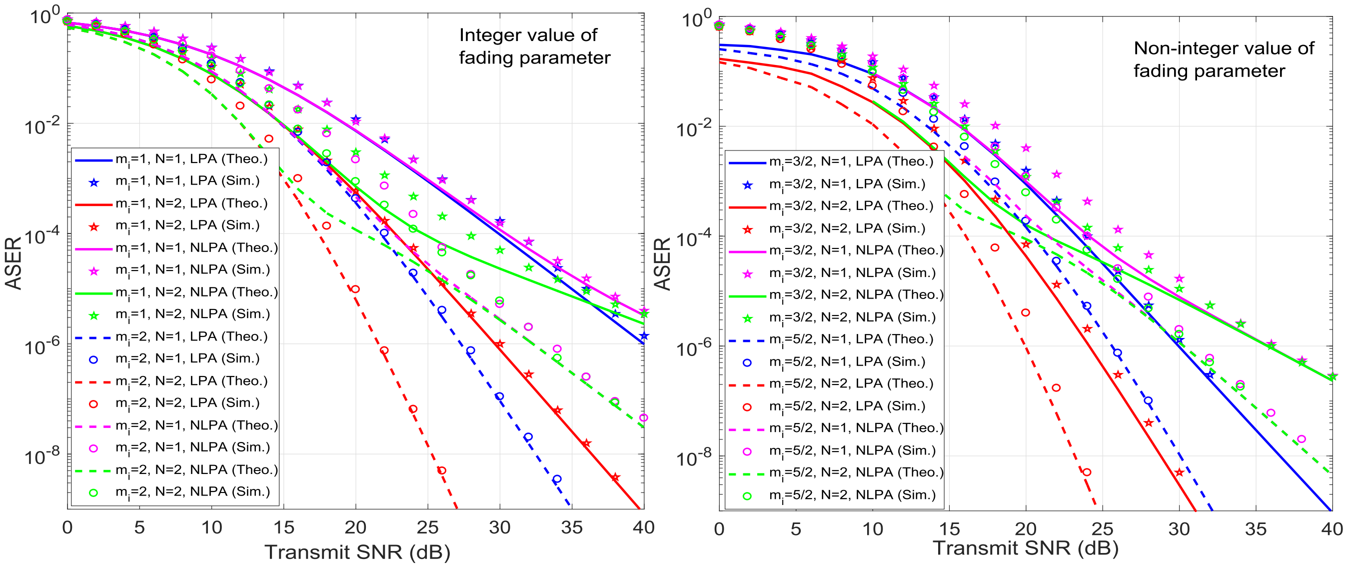

FIGURE 5. Comparison of theoretical and simulation results of ASER for 16-HQAM with imperfect CSI, and NLPA at the relays.

for different values of m_i and N with NLPA at the relays. From FIGURE 4 and FIGURE 5, it is observed that for all the considered cases, theoretical results match well with the simulation results which validates the derived theoretical results. Further, LB of the theoretical results is also justified as it is always below the simulation results. From FIGURE 4 and FIGURE 5, it is observed that for $m_i = 1$ and $N = 1$, approximately 0.5 dB SNR degradation is received to obtain ASER of 10^{-4} for the 16-HQAM when NLPA is considered over LPA at the relays, for perfect as well as imperfect CSI cases. For $m_i = 1$ and $N = 2$, for ASER of 10^{-4} for 16-HQAM, approx. 1.77 dB and 1.90 dB SNR degradation is observed for perfect CSI and imperfect CSI cases, respectively with NLPA over LPA at the relays. Further, for perfect CSI, keeping $m_i = 1$ and increasing N from 1 to 2, SNR gain of around 7.18 dB is achieved for 10^{-4} ASER with LPA consideration which is reduced to 5.80 dB with NLPA consideration. At high SNR, the ASER performance deteriorates further and negligible improvement in ASER performance is received for higher order QAM constellations with the increase in N, in presence of NLPA. For perfect CSI, keeping $N = 1$ and increasing m_i from 1 to 2, SNR gain of approx. 8.215 dB and 7.822 dB is observed for 10^{-4} ASER of 16-HQAM for LPA and NLPA, respectively at the relays. For non-integer valued fading parameter with perfect CSI, keeping $m_i = 3/2$ and increasing N from 1 to 2, SNR

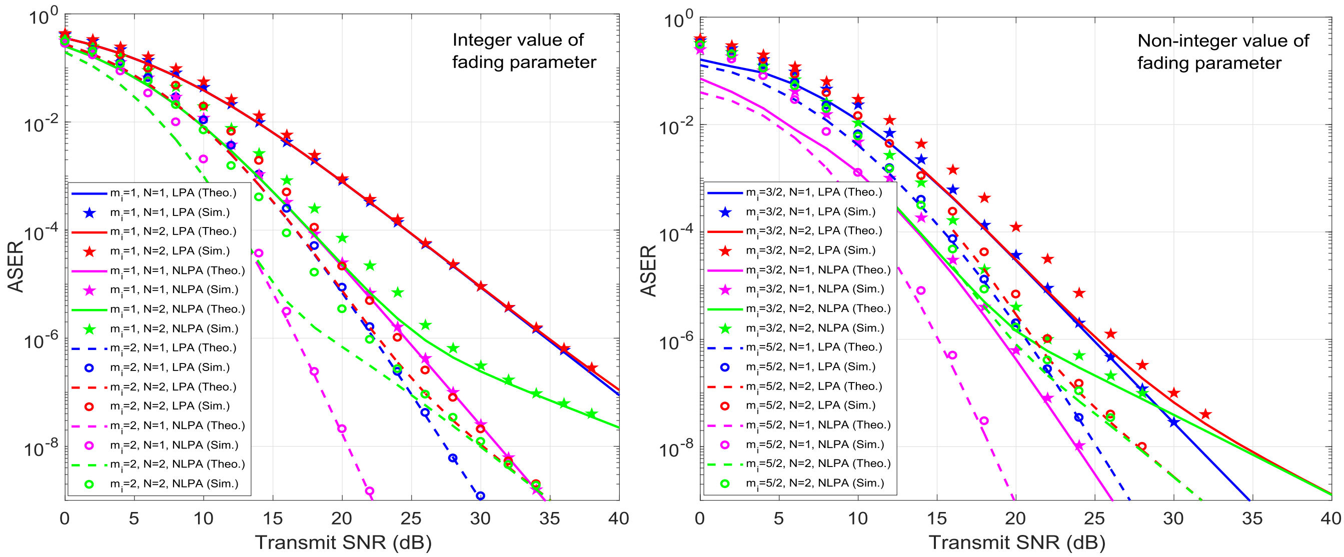

FIGURE 6. **Comparison of theoretical and simulation results of ASER for 4 × 2-RQAM with perfect CSI, and NLPA at the relays.**

gain of around 4.4 dB is achieved for 10^{-4} ASER with LPA consideration which is reduced to 2.4 dB with NLPA consideration. Further, for perfect CSI, keeping $N = 1$ and increasing m_i from 3/2 to 5/2, SNR gains of approx. 2.8 dB and 2.54 dB are observed for 10^{-4} ASER of 16-HQAM for LPA and NLPA, respectively at the relays.

Further, to achieve 10^{-4} ASER, approx. 3 dB SNR degradation is observed for imperfect CSI case ($\rho = 1$) over the perfect CSI case ($\rho \to \infty$), for all the combinations of m_i and N and for both the LPA and NLPA considerations. Thus, from the above discussion, it can be concluded that increase in fading parameter m_i provides higher SNR gain than increase in N specially in case of NLPA at the relays. In case of NLPA over LPA, SNR gain is reduced for all the combinations of m_i and N which reduces further for increasing constellation orders in medium and high SNR regime.

In FIGURE 6, comparison of theoretical and simulation results of ASER for 4×2-RQAM scheme with perfect CSI is illustrated for different values of m_i and N with NLPA at the relays. In FIGURE 6, only the perfect CSI case is considered since for imperfect CSI, similar ASER behavior is obtained however, with approx. 3 dB decrease in SNR than perfect CSI case for all the combinations of m_i and N. From FIGURE 6, it is observed that for all the considered cases, theoretical results match well with the simulation results which validates the derived theoretical results. Further, it is observed that keeping $m_i = 1$ and increasing N from 1 to 2, SNR gain of around 7.019 dB and 6.985 dB are achieved to obtain 10^{-4} ASER of 4×2-RQAM for the respective LPA and NLPA considerations at the relays. Further, keeping $N = 1$ and increasing m_i from 1 to 2, SNR gain of around 7.992 dB and 7.981 dB are achieved for ASER of 10^{-4} for 4×2-RQAM for both LPA and NLPA considerations at the relays, respectively.

In FIGURE 7, comparison of theoretical ASER results for 4-HQAM and 64-HQAM with respective SQAM schemes is shown for $m_i = 1$ and different values of N, by considering both perfect and imperfect CSI cases with NLPA at the relays. From FIGURE 7, it is observed that for all the investigated cases, ASER performance of 4-HQAM is slightly lower than 4-SQAM due to larger τ for HQAM with same α. However, for higher constellation order (M), HQAM outperforms SQAM due to higher values of α with relatively lower PAPR than SQAM [6], [13]. From FIGURE 7, it is observed that for $m_i = 1$ and $N = 1$, 4-SQAM provides approx. 0.15 dB SNR gain over 4-HQAM. However, with the increase in constellation points M, HQAM perform better than SQAM and for $m_i = 1$ and $N = 1$, 64-HQAM provides approx. 0.5 dB gain over 64-SQAM. Further, from FIGURE 7, it is clear that there is no impact of NLD on the ASER performance of HQAM and SQAM for lower order constellation $M = 4$. However, impact of NLD increases with the increase in M from 4 to 16 to 64 which obliterates the impact of relay selection for $M = 64$ (as can be seen from FIGURE 7.)

In FIGURE 8, theoretical results of ASER for 32-HQAM, 32-XQAM and 8×4-RQAM are compared for different values of m_i and N with perfect CSI and NLPA at the relays. It is observed that 32-XQAM provides improved ASER performance than 8×4-RQAM for all the considered cases due to its lower PAPR than RQAM scheme. Further, 32-HQAM outperforms the 32-XQAM for all the considered cases as observed in FIGURE 8. This shows the superiority of HQAM over the other modulation schemes. For $m_i = 1$ and $N = 1$, to obtain an ASER of 10^{-4}, 32-HQAM provides around 0.16 dB and 1.29 dB SNR gain over 32-XQAM and 8×4-RQAM schemes, respectively in the presence of LPA. However, for $m_i = 1$ and $N = 1$, to obtain an ASER of 10^{-4}, 32-HQAM provides around 0.90 dB and 4.9 dB SNR gain over 32-XQAM and 8×4-RQAM schemes, respectively in the presence of NLPA. Thus, for $m_i = 1$ and $N = 1$, around 8.87 dB decrease in the SNR is obtained to achieve an

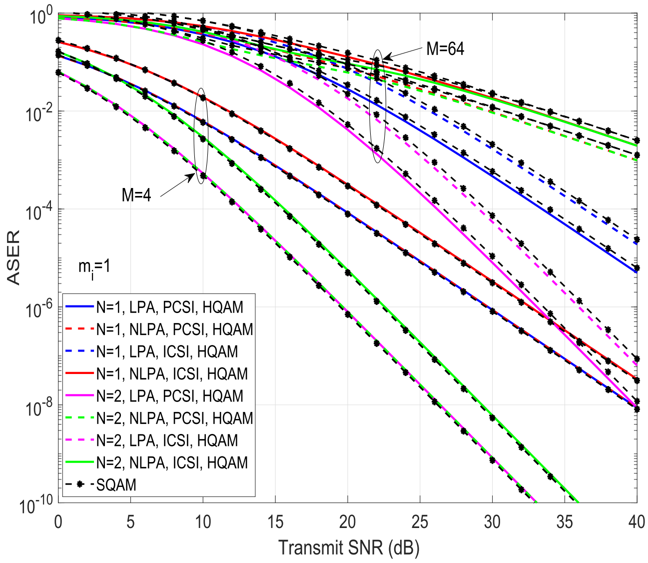

FIGURE 7. Comparison of theoretical results of ASER for 4-HQAM and 64-HQAM with respective SQAM schemes, for $m_i = 1$ in perfect and imperfect CSI conditions with NLPA at the relays.

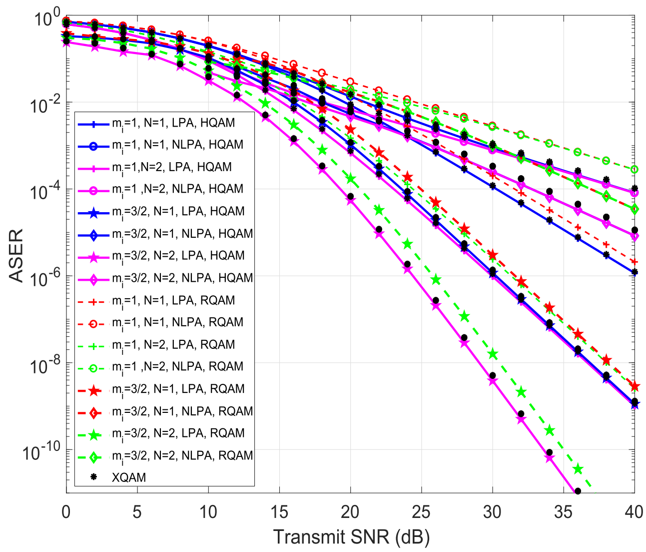

FIGURE 8. Comparative analysis of theoretical results of ASER for 32-HQAM, 32-XQAM and 8 × 4-RQAM schemes in perfect CSI conditions with NLPA at the relays.

ASER of 10^{-4} for 32-HQAM with NLPA. Further, keeping $N = 1$ and increasing m_i from 1 to 3/2, respective SNR gain of around 6.65 dB and 6.43 dB are obtained to achieve 10^{-4} ASER of 32-HQAM in the absence and presence of NLPA. However, keeping $m_i = 1$ and increasing N from 1 to 2, respective SNR gain of around 7.25 dB and 0.07 dB are obtained at ASER of 10^{-4} for 32-HQAM in both the absence and presence of NLPA. Thus, increase in m_i provides significant gain in ASER performance as compared to the increase in N for all the considered cases (especially in case of NLPA where the impact of relay selection is negligible for the higher order constellations.)

VII. CONCLUSION

In this paper, closed-form expressions of the outage probability, and ASER for general order HQAM, general order RQAM and 32-XQAM schemes over Nakagami-m fading links with both integer as well as non-integer fading parameter have been derived and compared for the considered multi-relay system. Further, asymptotic analysis on the outage probability has been carried out to obtain the diversity order of the considered system. Impact of the fading parameter, number of relays, NLD and CEE on the system performance have also been illustrated. Due to the high data-rate with optimum spectral efficiency and their applicability for both the even and odd power of 2 constellations, these higher order QAM schemes are expected to design more reliable, flexible and efficient broadcasting and mobile communication systems.

APPENDIX A

LB of the CDF of indirect $S - R_n - D$ link can be expressed as

$$\begin{aligned} F_{\gamma^*_{srnd}}(\gamma_{th}) &= \mathcal{P}\Big(\underset{n\in\{1,\ldots,N\}}{\text{argmax}}\{\gamma^{UB}_{sr_nd}\} \leq \gamma_{th}\Big) \\ &= \mathcal{P}\Big(\underset{n\in\{1,\ldots,N\}}{\text{argmax}} \min\Big(\frac{\hat{\gamma}_{sr_n}}{L_{r_nd}}, \gamma^{pa}, \frac{\hat{\gamma}_{r_nd}}{L_{sr_n}}\Big) \leq \gamma_{th}\Big) \\ &= \Pi^N_{n=1}\Big\{1 - [1 - F_{\hat{\gamma}_{sr_n}}(L_{r_nd}\gamma_{th})][1 - F_{\gamma^{pa}}(\gamma_{th})] \\ &\quad [1 - F_{\hat{\gamma}_{r_nd}}(L_{sr_n}\gamma_{th})]\Big\}. \end{aligned} \tag{24}$$

For arbitrary value of fading parameter, CDF and PDF of a Nakagami-m distributed link can be given as [33]

$$\begin{aligned} F_{\gamma_i}(x) &= \Big[1 - \frac{1}{\Gamma(m)}\Gamma\Big(m_i, \frac{m_i x}{\bar{\gamma}_i}\Big)\Big]u(x), \\ f_{\gamma_i}(x) &= \Big[\frac{1}{\Gamma(m_i)}\Big(\frac{m_i}{\bar{\gamma}_i}\Big)^{m_i} x^{m_i - 1} e^{-\frac{m_i x}{\bar{\gamma}_i}}\Big]u(x), \end{aligned} \tag{25}$$

respectively, where $\bar{\gamma}_i$ represents the average SNR of the i^{th} link. Also, a fixed SNR of the NLPA is considered and hence, $\bar{\gamma}_{pa} = \gamma_{pa}$. Thus, its CDF can be given as $F_{\gamma_{pa}}(\gamma_{th}) = u(\gamma_{th} - \bar{\gamma}_{pa})$ [24]. Further, considering identical relays, substituting the CDF of the i^{th} link from (25) in (24) and after some mathematical computations, we get

$$\begin{aligned} &F^*_{\gamma_{srnd}}(\gamma_{th}) \\ &= \Big[1 + \sum_{n=1}^{N}\binom{N}{n}(-1)^n\Bigg(\frac{\Gamma\Big(m_{sr_n}, \frac{m_{sr_n}}{\bar{\hat{\gamma}}_{sr_n}}L_{r_nd}\gamma_{th}\Big)}{\Gamma(m_{sr_n})}\Bigg)^n \\ &\quad \times \Bigg(\frac{\Gamma\Big(m_{r_nd}, \frac{m_{r_nd}}{\bar{\hat{\gamma}}_{r_nd}}L_{sr_n}\gamma_{th}\Big)}{\Gamma(m_{r_nd})}\Bigg)^n u(\bar{\gamma}_{pa} - \gamma_{th})\Big]u(\gamma_{th}). \end{aligned} \tag{26}$$

Proof of Theorem 1:

A. INTEGER VALUED FADING PARAMETER

For the integer valued fading parameter, upper incomplete gamma function can be expanded as [34, (8.352.7)]. Thus, the CDF of the Nakagami-m distributed i^{th} link can be expressed as

$$F_{\gamma_i}(x) = \Big[1 - e^{-(\frac{m_i x}{\bar{\gamma}_i})} \sum_{l=0}^{m_i-1} \frac{1}{l!}\Big(\frac{m_i x}{\bar{\gamma}_i}\Big)^l\Big]u(x). \quad (27)$$

To solve (26), upper incomplete gamma function can be expanded as [34, (8.352.7)]

$$\left(\frac{\Gamma(m_i, \eta\gamma)}{\Gamma(m_i)}\right)^n = e^{-n\eta\gamma}\Big[\sum_{\mu=0}^{m_i-1} \frac{(\eta\gamma)^\mu}{\mu!}\Big]^n. \quad (28)$$

The multinomial present in (28) can be expanded as $\Big[\sum_{\mu=0}^{m_i-1}(\delta_\mu \gamma^\mu)\Big]^n = \sum_{\mu=0}^{n(m_i-1)} \varphi_\mu^n \gamma^\mu$, where φ_μ^n can be recursively calculated as $\varphi_0^n = (\delta_0)^n$, $\varphi_1^n = n(\delta_1)$, $\varphi_{n(m_i-1)}^n = (\delta_{m_i-1})^n$ for $0 \le \mu \le n(m_i-1)$, $\varphi_\mu^n = \frac{1}{\mu\delta_0}\sum_{q=1}^{\mu}\Big[(qn-\mu+q)\delta_q\varphi_{\mu-q}^n\Big]$ for $2 \le \mu \le (m_i-1)$ and $\varphi_\mu^n = \frac{1}{\mu\delta_0}\sum_{q=1}^{m_i-1}\Big[(qn-\mu+q)\delta_q\varphi_{\mu-q}^n\Big]$ for $m_i \le \mu \le n(m_i-1)$ where $\delta_\mu = \frac{\eta^\mu}{\mu!}$ [6]. Thus, (26) can be further written as

$$F^*_{\gamma_{srnd}}(\gamma_{th}) = \Big[1 + \sum_{n=1}^{N}\binom{N}{n}(-1)^n \sum_{j=0}^{n(m_{sr_n}-1)} \sum_{k=0}^{n(m_{r_nd}-1)} \varphi_j^n \times \varphi_k^n \eta_1^j \eta_2^k \gamma_{th}^{j+k} e^{-C_2\gamma_{th}} u(\bar{\gamma}_{pa} - \gamma_{th})\Big]u(\gamma_{th}). \quad (29)$$

where $\eta_1 = \Big(\frac{m_{srn}L_{rnd}}{\bar{\gamma}_{srn}}\Big)$ and $\eta_2 = \Big(\frac{m_{rnd}L_{srn}}{\bar{\gamma}_{rnd}}\Big)$.

Substituting the PDF of $S-D$ link from (25) and CDF of $S-R_n-D$ link from (29) in (12), we get

$$\mathcal{P}_{out}^{LB}(\gamma_{th}) = F_{\gamma_{sd}}(\gamma_{th}) + \sum_{n=1}^{N}\binom{N}{n}(-1)^n \sum_{j=0}^{n(m_{sr_n}-1)} \times \sum_{k=0}^{n(m_{r_nd}-1)} \varphi_j^n\varphi_k^n\eta_1^j\eta_2^k e^{-C_2\gamma_{th}} \frac{C_3^{m_{sd}}}{\Gamma(m_{sd})} \times \int_{\gamma_{max}}^{\gamma_{th}} x^{m_{sd}-1}(\gamma_{th}-x)^{j+k} e^{-(C_3-C_2)x}dx. \quad (30)$$

Further, solving the required integral with the help of [34, (3.351)], closed-form expression for the LB of outage probability can be expressed as (13).

B. NON-INTEGER VALUED FADING PARAMETER

For non-integer valued fading parameter, upper incomplete gamma function can be expanded as [35, (36)]. Thus, the CDF of the Nakagami-m distributed i^{th} link can be expressed as

$$F_{\gamma_i}(x) = e^{-\frac{m_i}{\bar{\gamma}_i}x}\sum_{g=0}^{\infty}\frac{1}{\Gamma(m_i+g+1)}\Big(\frac{m_i x}{\bar{\gamma}_i}\Big)^{(m_i+g)}u(x). \quad (31)$$

To solve (26), upper incomplete gamma function can be expanded as [35, (36)]

$$\left(\frac{\Gamma(m_i,\Theta\gamma)}{\Gamma(m_i)}\right)^n = \Big[1 - \sum_{g=0}^{\infty}\frac{e^{-\Theta\gamma}}{\Gamma(m_i+g+1)}(\Theta\gamma)^{(m_i+g)}\Big]^n. \quad (32)$$

Using the binomial series expansion and invoking [34, (0.314)], multinomial presents in (32) can be expanded as $\Big[\sum_{\upsilon=0}^{\infty}(\theta_\upsilon\gamma^\upsilon)\Big]^n = \sum_{\upsilon=0}^{\infty}\psi_\upsilon^n\gamma^\upsilon$, where ψ_υ^n can be recursively calculated as $\psi_0^n = (\theta_0)^n$, $\psi_\upsilon^n = \frac{1}{\upsilon\theta_0}\sum_{z=1}^{\upsilon}(zn-\upsilon+z)\theta_z\psi_{\upsilon-z}^n$ for $\upsilon \ge 1$ where $\theta_\upsilon = \frac{1}{\Gamma(m_i+\upsilon+1)}\Theta^{(m_i+\upsilon)}$. Thus, (26) can be further written as

$$F^*_{\gamma_{srnd}}(\gamma_{th}) = \Big[1 + \sum_{n=1}^{N}\binom{N}{n}\sum_{p=0}^{n}\binom{n}{p}\sum_{p_1=0}^{n}\binom{n}{p_1}(-1)^{(n+p+p_1)} \times \sum_{\upsilon_1=0}^{\infty}\sum_{\upsilon_2=0}^{\infty}\psi_{\upsilon_1}^p\psi_{\upsilon_2}^{p_1}\gamma_{th}^{(\upsilon_1+\upsilon_2+pm_{sr_n}+p_1m_{r_nd})} \times e^{-(p\eta_1+p_1\eta_2)\gamma_{th}}u(\bar{\gamma}_{pa}-\gamma_{th})\Big]u(\gamma_{th}). \quad (33)$$

Substituting the PDF of $S-D$ link from (25) and CDF of $S-R_n-D$ link from (33) in (12), we get

$$\mathcal{P}_{out}^{LB}(\gamma_{th}) = F_{\gamma_{sd}}(\gamma_{th}) + \Big[\frac{C_3^{m_{sd}}}{\Gamma(m_{sd})}\sum_{n=1}^{N}\binom{N}{n}\sum_{p=0}^{n}\binom{n}{p} \times \sum_{p_1=0}^{n}\binom{n}{p_1}(-1)^{(n+p+p_1)}\sum_{\upsilon_1=0}^{\infty}\sum_{\upsilon_2=0}^{\infty}\psi_{\upsilon_1}^p\psi_{\upsilon_2}^{p_1} \times \sum_{i_1=0}^{\infty}(-1)^{i_1}\binom{\upsilon_1+\upsilon_2+pm_{sr_n}+p_1m_{r_nd}}{i_1} \times e^{-(p\eta_1+p_1\eta_2)\gamma_{th}}\gamma_{th}^{(\upsilon_1+\upsilon_2+pm_{sr_n}+p_1m_{r_nd}-i_1)} \times \int_{\gamma_{max}}^{\gamma_{th}} x^{(msd+i_1-1)}e^{-(C_3-(p\eta_1+p_1\eta_2))x}dx. \quad (34)$$

Further, solving the required integral with the help of [34, (3.351.1)], closed-form expression for the LB of outage probability can be expressed as (14).

APPENDIX B
PROOF OF THEOREM

For asymptotic analysis, outage probability expression is approximated at high SNR ($\gamma_0 \to \infty$) which corresponds to ($\bar{\gamma}_i \to \infty$). To do this, high SNR approximation of the i^{th} link's CDF is substituted in (24) by incorporating the high SNR approximation of lower incomplete gamma function (for integer as well as non-integer valued fading parameters) as $\Upsilon(m,z) \underset{z\to 0}{\approx} (\frac{z^m}{m})$ [36]. Thus, (24) can be modified as

$$F^*_{\gamma_{srnd}}(\gamma_{th}) \approx \Big[1 + \sum_{n=1}^{N}\binom{N}{n}(-1)^n \times \Big(1 - \frac{(\eta_1\gamma_{th})^{m_{srn}}}{m_{sr_n}!}u(\gamma_{th})\Big)^n\Big(1 - \frac{(\eta_2\gamma_{th})^{m_{r_nd}}}{m_{r_nd}!}u(\gamma_{th})\Big)^n \times u(-\gamma_{th}+\bar{\gamma}_{pa})\Big]u(\gamma_{th}). \quad (35)$$

At high SNR, PDF of the $S-D$ link can be approximated as

$$f_{\gamma_{sd}}(x) \approx \Big(\frac{m_{sd}}{\bar{\gamma}_{sd}}\Big)^{m_{sd}}\frac{x^{m_{sd}-1}}{\Gamma(m_{sd})}u(x). \quad (36)$$

Thus, substituting $f_{\gamma_{sd}}(x)$ from (36) in (12) along with the approximated value of $F_{\gamma^*_{srnd}}(\gamma_{th} - x)$ from (35), outage probability can be approximated as

$$\mathcal{P}_{out}^{asym}(\gamma_{th}) \approx \sum_{n=0}^{N}\sum_{j=0}^{n}\sum_{k=0}^{n}\binom{N}{n}\binom{n}{j}\binom{n}{k}(-1)^{n+j+k} \times \frac{C_3^{m_{sd}}}{\Gamma(m_{sd})}\frac{\eta_1^{jm_{srn}}}{(m_{sr_n}!)^j}\frac{\eta_2^{km_{r_nd}}}{(m_{r_nd}!)^k} \int_{\gamma_{max}}^{\gamma_{th}} x^{m_{sd}-1}(\gamma_{th}-x)^{(jm_{sr_n}+km_{r_nd})}dx. \quad (37)$$

Case 1: For $\gamma_{th} < \bar{\gamma}_{pa}$

Solving (37) for $\gamma_{th} < \bar{\gamma}_{pa}$, closed-form expression of the asymptotic outage probability is shown in (15).

Case 2: For $\gamma_{th} > \bar{\gamma}_{pa}$

Closed-form expression of the asymptotic outage probability can be given as (16).

APPENDIX C

The conditional SEP expression for M-ary HQAM scheme in AWGN channel can be given as [13]

$$\mathcal{P}_s^H(e|\gamma) = Q(\sqrt{\alpha\gamma})\Big[\tau - 2\tau_c Q\Big(\sqrt{\alpha\gamma/3}\Big)\Big] + 2/3\tau_c Q^2\Big(\sqrt{2\alpha\gamma/3}\Big), \quad (38)$$

where α, τ and τ_c are constants defined in [13] and their different values are used to select various HQAM constellations. Substituting the Gaussian Q-function $Q(z) = \frac{1}{2}[1 - \mathrm{erf}(\frac{z}{\sqrt{2}})]$ in (38), we obtain

$$\mathcal{P}_s^H(e|\gamma) = \Big(1 - \mathrm{erf}\Big(\sqrt{\tfrac{\alpha\gamma}{2}}\Big)\Big)\Big[\tfrac{\tau}{2} - \tfrac{\tau_c}{2}\Big(1 - \mathrm{erf}\Big(\sqrt{\tfrac{\alpha\gamma}{6}}\Big)\Big)\Big] + \tfrac{\tau_c}{6}\Big(1 - \mathrm{erf}\Big(\sqrt{\tfrac{\alpha\gamma}{3}}\Big)\Big)^2. \quad (39)$$

Utilizing (a) first order derivative of error function, $\frac{d}{dz}\mathrm{erf}(z) = \frac{2}{\sqrt{\pi}}e^{-z^2}$ [37, (7.1.19)], (b) expansion of error function, $\mathrm{erf}(z) = \frac{2z}{\sqrt{\pi}}e^{-z^2}\,{}_1F_1(1, \frac{3}{2}, z^2)$ [37, (7.1.21)], first order derivative of (39) can be expressed as

$$\mathcal{P}'^H_s(e|\gamma) = \gamma^{-1/2}\Big[\frac{1}{2}\sqrt{\frac{\alpha}{2\pi}}(\tau_c - \tau)e^{-\frac{\alpha\gamma}{2}} - \frac{\tau_c}{3}\sqrt{\frac{\alpha}{3\pi}} \times e^{-\frac{\alpha\gamma}{3}} + \frac{\tau_c}{2}\sqrt{\frac{\alpha}{6\pi}}e^{-\frac{\alpha\gamma}{6}}\Big] + \frac{2\tau_c\alpha}{9\pi}e^{-\frac{2\alpha}{3}\gamma}\,{}_1F_1\Big(1; \frac{3}{2}; \frac{\alpha}{3}\gamma\Big) - \frac{\tau_c\alpha e^{-\frac{2\alpha}{3}\gamma}}{2\sqrt{3}\pi}\Big[{}_1F_1\Big(1; \frac{3}{2}; \frac{\alpha}{2}\gamma\Big) + {}_1F_1\Big(1; \frac{3}{2}; \frac{\alpha}{6}\gamma\Big)\Big]. \quad (40)$$

Proof of Theorem 3:

A. INTEGER VALUED FADING PARAMETER

Substituting the respective values of $\mathcal{P}'^H_s(e|\gamma)$ and $\mathcal{P}_{out}^{LB}(\gamma)$ from (40) and (13) in (17) and solving the required integrals with the help of [34, (3.351.1), (3.351.2), (6.455.1), (6.455.2)], closed-form expression for the ASER of general order HQAM can be expressed as (18).

B. NON-INTEGER VALUED FADING PARAMETER

Substituting the respective values of $\mathcal{P}'^H_s(e|\gamma)$ and $\mathcal{P}_{out}^{LB}(\gamma)$ from (40) and (14) in (17) and solving the required integrals with the help of [34, (3.351.1), (3.351.2), (3.351.3), (6.455.1)], closed-form expression for the ASER of general order HQAM can be expressed as (19).

APPENDIX D

For $M_I \times M_Q$-ary QAM scheme, a generalized conditional SEP expression for AWGN channel can be given as [2]

$$\mathcal{P}_s^R(e|\gamma) = 2\Big[p_0 Q(a_0\sqrt{\gamma})(1 - 2q_0 Q(b_0\sqrt{\gamma})) + q_0 Q(b_0\sqrt{\gamma})\Big], \quad (41)$$

where $p_0 = 1 - (1/M_I)$, $q_0 = 1 - (1/M_Q)$, $a_0 = \sqrt{6/((M_I^2 - 1) + (M_Q^2 - 1)\lambda^2)}$, $b_0 = \lambda a_0$, and $\lambda = d_Q/d_I$ represents the ratio of quadrature and in-phase decision distances. Also, M_I and M_Q represent respectively the in-phase and quadrature phase constellation points. Further, substituting $Q(z) = \frac{1}{2}[1 - \mathrm{erf}(\frac{z}{\sqrt{2}})]$ in (40) and using [37, (7.1.21)], first order derivative of (41) can be expressed as

$$\mathcal{P}'^R_s(e|\gamma) = \gamma^{-\frac{1}{2}}\Big[\frac{a_0p_0(q_0-1)}{\sqrt{2\pi}}e^{-\frac{a_0^2\gamma}{2}} + \frac{b_0(p_0-1)q_0}{\sqrt{2\pi}}e^{-\frac{b_0^2\gamma}{2}}\Big] - \frac{a_0b_0p_0q_0}{\pi}e^{-\frac{(a_0^2+b_0^2)\gamma}{2}} \times \Big[{}_1F_1\Big(1; 1.5; \frac{a_0^2\gamma}{2}\Big) + {}_1F_1\Big(1; 1.5; \frac{b_0^2\gamma}{2}\Big)\Big]. \quad (42)$$

Proof of Theorem 4:

A. INTEGER VALUED FADING PARAMETER

Substituting $\mathcal{P}'^R_s(e|\gamma)$ and $\mathcal{P}_{out}^{LB}(\gamma)$ from (42) and (13), respectively in (17) and solving the required integrals with the help of [34, (3.351.1), (3.351.2), (6.455.1), (6.455.2)], final expression for the ASER of general order RQAM scheme can be expressed as (20).

B. NON-INTEGER VALUED FADING PARAMETER

Substituting $\mathcal{P}'^R_s(e|\gamma)$ and $\mathcal{P}_{out}^{LB}(\gamma)$ from (42) and (14), respectively in (17) and solving the required integrals with the help of [34, (3.351.1), (3.351.2), (3.351.3) (6.455.1)], final expression for the ASER of general order RQAM scheme can be expressed as (21).

APPENDIX E

The conditional SEP expression for 32-XQAM scheme in AWGN channel can be given as [6]

$$\mathcal{P}_s^X(e|\gamma) = \tfrac{1}{8}\Big[26Q(\sqrt{2\chi\gamma}) + Q(2\sqrt{\chi\gamma}) - 23Q^2(\sqrt{2\chi\gamma})\Big], \quad (43)$$

where $\chi = 48/(31M - 32)$. The first order derivative of (43) can be derived as

$$\mathcal{P}'^{X}_{s}(e|\gamma) = -\frac{1}{8}\Big[\frac{3}{2}\sqrt{\frac{\chi}{\pi}}\frac{e^{-\chi\gamma}}{\sqrt{\gamma}} + \sqrt{\frac{\chi}{2\pi}}\frac{e^{-2\chi\gamma}}{\sqrt{\gamma}} + \frac{23\chi}{\pi}e^{-2\chi\gamma}\,{}_1F_1\Big(1;\frac{3}{2};\chi\gamma\Big)\Big]. \quad (44)$$

Proof of Theorem 5:

A. INTEGER VALUED FADING PARAMETER

Substituting the respective values of $\mathcal{P}'^{X}_{s}(e|\gamma)$ and $\mathcal{P}^{LB}_{out}(\gamma)$ from (44) and (13) in (17), and solving the required integrals using [34, (3.351.1), (3.351.2), (6.455.1), (6.455.2)], final expression for the ASER of 32-XQAM can be expressed as (22).

B. NON-INTEGER VALUED FADING PARAMETER

Substituting the respective values of $\mathcal{P}'^{X}_{s}(e|\gamma)$ and $\mathcal{P}^{LB}_{out}(\gamma)$ from (44) and (14) in (17), and solving the required integrals using [34, (3.351.1), (3.351.2), (3.351.3), (6.455.1)], final expression for the ASER of 32-XQAM can be expressed as (23).

REFERENCES

[1] Y. Yang, H. Hu, J. Xu, and G. Mao, "Relay technologies for WiMAX and LTE-advanced mobile systems," *IEEE Commun. Mag.*, vol. 47, no. 10, pp. 100–105, Oct. 2009.

[2] D. Dixit and P. R. Sahu, "Performance analysis of rectangular QAM with SC receiver over Nakagami-*m* fading channels," *IEEE Commun. Lett.*, vol. 18, no. 7, pp. 1262–1265, Jul. 2014.

[3] S. Kim, H. W. Kim, K. Kang, and D. S. Ahn, "Performance enhancement in future mobile satellite broadcasting services," *IEEE Commun. Mag.*, vol. 46, no. 7, pp. 118–124, Jul. 2008.

[4] P. K. Vitthaladevuni, M.-S. Alouini, and J. C. Kieffer, "Exact BER computation for cross QAM constellations," *IEEE Trans. Wireless Commun.*, vol. 4, no. 6, pp. 3039–3050, Nov. 2005.

[5] X.-C. Zhang, H. Yu, and G. Wei, "Exact symbol error probability of cross-QAM in AWGN and fading channels," *EURASIP J. Wireless Commun. Netw.*, vol. 2010, Dec. 2010, Art. no. 917954.

[6] N. Kumar, P. K. Singya, and V. Bhatia, "ASER analysis of hexagonal and rectangular QAM schemes in multiple-relay networks," *IEEE Trans. Veh. Technol.*, vol. 67, no. 2, pp. 1815–1819, Feb. 2018.

[7] P. K. Singya, N. Kumar, and V. Bhatia, "Impact of imperfect CSI on ASER of hexagonal and rectangular QAM for AF relaying network," *IEEE Commun. Lett.*, vol. 22, no. 2, pp. 428–431, Feb. 2018.

[8] P. K. Singya, N. Kumar, V. Bhatia, and F. A. Khan, "Performance analysis of OFDM based 3-hop AF relaying network over mixed Rician/Rayleigh fading channels," *AEU-Int. J. Electron. Commun.*, vol. 93, pp. 337–347, Sep. 2018.

[9] K. N. Pappi, A. S. Lioumpas, and G. K. Karagiannidis, "θ-QAM: A parametric quadrature amplitude modulation family and its performance in AWGN and fading channels," *IEEE Trans. Commun.*, vol. 58, no. 4, pp. 1014–1019, Apr. 2010.

[10] P. K. Vitthaladevuni and M.-S. Alouini, "BER computation of 4/M-QAM hierarchical constellations," *IEEE Trans. Broadcast.*, vol. 47, no. 3, pp. 228–239, Sep. 2001.

[11] D. Dixit and P. R. Sahu, "Performance of dual-hop DF relaying systems with QAM schemes over mixed η-μ and κ-μ fading channels," *Trans. Emerg. Telecommun. Technol.*, vol. 28, no. 11, p. e3179, Nov. 2017.

[12] J. P. Peña-Martín, J. M. Romero-Jerez, and C. Tellez-Labao, "Performance of selection combining diversity in $\eta - \mu$ fading channels with integer values of μ," *IEEE Trans. Veh. Technol.*, vol. 64, no. 2, pp. 834–839, Feb. 2015.

[13] L. Rugini, "Symbol error probability of hexagonal QAM," *IEEE Commun. Lett.*, vol. 20, no. 8, pp. 1523–1526, Aug. 2016.

[14] S.-J. Park, "Performance analysis of triangular quadrature amplitude modulation in AWGN channel," *IEEE Commun. Lett.*, vol. 16, no. 6, pp. 765–768, Jun. 2012.

[15] L. Yang, K. Qaraqe, E. Serpedin, and M.-S. Alouini, "Performance analysis of amplify-and-forward two-way relaying with co-channel interference and channel estimation error," *IEEE Trans. Commun.*, vol. 61, no. 6, pp. 2221–2231, Jun. 2013.

[16] P. Aquilina and T. Ratnarajah, "Performance analysis of IA techniques in the MIMO IBC with imperfect CSI," *IEEE Trans. Commun.*, vol. 63, no. 4, pp. 1259–1270, Apr. 2015.

[17] M. Seyfi, S. Muhaidat, and J. Liang, "Amplify-and-forward selection cooperation over Rayleigh fading channels with imperfect CSI," *IEEE Trans. Wireless Commun.*, vol. 11, no. 1, pp. 199–209, Jan. 2012.

[18] L. Wang, Y. Cai, and W. Yang, "On the finite-SNR DMT of two-way AF relaying with imperfect CSI," *IEEE Wireless Commun. Lett.*, vol. 1, no. 3, pp. 161–164, Jun. 2012.

[19] S. Bharadwaj and N. B. Mehta, "Accurate performance analysis of single and opportunistic AF relay cooperation with imperfect cascaded channel estimates," *IEEE Trans. Commun.*, vol. 61, no. 5, pp. 1764–1775, May 2013.

[20] C.-L. Wang and J.-Y. Chen, "Power allocation and relay selection for AF cooperative relay systems with imperfect channel estimation," *IEEE Trans. Veh. Technol.*, vol. 65, no. 9, pp. 7809–7813, Sep. 2016.

[21] P. K. Singya, N. Kumar, and V. Bhatia, "Mitigating NLD for wireless networks: Effect of nonlinear power amplifiers on future wireless communication networks," *IEEE Microw. Mag.*, vol. 18, no. 5, pp. 73–90, Jul./Aug. 2017.

[22] N. Kumar, P. K. Singya, and V. Bhatia, "Performance analysis of orthogonal frequency division multiplexing-based cooperative amplify-and-forward networks with non-linear power amplifier over independently but not necessarily identically distributed Nakagami-m fading channels," *IET Commun.*, vol. 11, no. 7, pp. 1008–1020, May 2017.

[23] N. Kumar, S. Sharma, and V. Bhatia, "Performance analysis of OFDM-based nonlinear AF multiple-relay systems," *IEEE Wireless Commun. Lett.*, vol. 6, no. 1, pp. 122–125, Feb. 2017.

[24] C. A. R. Fernandes, D. B. D. Costa, and A. L. F. D. Almeida, "Performance analysis of cooperative amplify-and-forward orthogonal frequency division multiplexing systems with power amplifier non-linearity," *IET Commun.*, vol. 8, no. 18, pp. 3223–3233, 2014.

[25] D. E. Simmons and J. P. Coon, "Two-way OFDM-based nonlinear amplify-and-forward relay systems," *IEEE Trans. Veh. Technol.*, vol. 65, no. 5, pp. 3808–3812, May 2016.

[26] P. K. Singya, N. Kumar, and V. Bhatia, "Performance analysis of AF OFDM system using multiple relay in presence of nonlinear-PA over inid Nakagami-m fading," *Int. J. Commun. Syst.*, vol. 31, no. 1, pp. 1–15, Jan. 2018.

[27] E. Balti and M. Guizani, "Impact of non-linear high-power amplifiers on cooperative relaying systems," *IEEE Trans. Commun.*, vol. 65, no. 5, pp. 4163–4175, Jul. 2017.

[28] E. Balti, M. Guizani, B. Hamdaoui, and B. Khalfi, "Mixed RF/FSO relaying systems with hardware impairments," in *Proc. IEEE Global Commun. Conf. (GLOBECOM)*, Dec. 2017, pp. 1–6.

[29] N. Maletić, M. Čabarkapa, and N. Nešković, "Performance of fixed-gain amplify-and-forward nonlinear relaying with hardware impairments," *Int. J. Commun. Syst.*, vol. 30, no. 6, p. e3102, Apr. 2017.

[30] D. Dardari, V. Tralli, and A. Vaccari, "A theoretical characterization of nonlinear distortion effects in OFDM systems," *IEEE Trans. Commun.*, vol. 48, no. 10, pp. 1755–1764, Oct. 2000.

[31] C. Wang, T. C.-K. Liu, and X. Dong, "Impact of channel estimation error on the performance of amplify-and-forward two-way relaying," *IEEE Trans. Veh. Technol.*, vol. 61, no. 3, pp. 1197–1207, Mar. 2012.

[32] M. Abdelaziz and T. A. Gulliver, "Triangular constellations for adaptive modulation," *IEEE Trans. Commun.*, vol. 66, no. 2, pp. 756–766, Feb. 2018.

[33] M.-S. Alouini and A. J. Goldsmith, "Adaptive modulation over Nakagami fading channels," *Wireless Pers. Commun.*, vol. 13, nos. 1–2, pp. 119–143, 2000.

[34] I. Gradshteyn and I. Ryzhik, *Table of Integrals, Series, and Products*, 6th ed. New York, NY, USA: Academic, 2000.

[35] E. Soleimani-Nasab, M. Matthaiou, and M. Ardebilipour, "Multi-relay MIMO systems with OSTBC over Nakagami-*m* fading channels," *IEEE Trans. Veh. Technol.*, vol. 62, no. 8, pp. 3721–3736, Oct. 2013.

[36] N. Kumar and V. Bhatia, "Exact ASER analysis of rectangular QAM in two-way relaying networks over Nakagami-*m* fading channels," *IEEE Wireless Commun. Lett.*, vol. 5, no. 5, pp. 548–551, Oct. 2016.
[37] M. Abramowitz and I. A. Stegun, *Handbook of Mathematical Functions: With Formulas, Graphs, and Mathematical Tables*, 9th ed. New York, NY, USA: Dover, 1970.

PRAVEEN K. SINGYA (S'18) received the B.E. degree in electronics and communication engineering from Jabalpur Engineering College, Jabalpur, India, in 2012, and the M.Tech. degree in communication system engineering from VNIT, Nagpur, India, in 2014. He is currently pursuing the Ph.D. degree with IIT Indore, Indore, India. His research interests include the design and the performance analysis of various cooperative networks over various fading channels.

NAGENDRA KUMAR (M'19) received the M.Tech. degree in electronics and communication engineering from the Jaypee University of Engineering and Technology, Guna, India, in 2012, and the Ph.D. degree from IIT Indore, India, in 2017. He is currently an Assistant Professor with the National Institute of Technology Jamshedpur, Jamshedpur, India. His research interests include the performance analysis of various cooperative diversity and relay networks.

VIMAL BHATIA (SM'12) received the Ph.D. degree from the Institute for Digital Communications, The University of Edinburgh, Edinburgh, U.K., in 2005. During the Ph.D. degree, he has also received the IEE Fellowship for collaborative research on OFDM with Prof. Falconer from the Department of Systems and Computer Engineering, Carleton University, Ottawa, ON, Canada. He is a Young Faculty Research Fellow of MeitY. He is currently a Professor with IIT Indore, Indore, India. He has more than 165 Publications. He has 11 patents filed. His research interest includes the broader area of non-Gaussian non-parametric signal processing with applications to communications. He is a reviewer of the IEEE, Elsevier, Wiley, Springer, and IET. He is currently a certified SCRUM Master. He is also the General Vice-Chair of the IEEE ANTS 2017 and the General Co-Chair of the IEEE ANTS 2018.

MOHAMED-SLIM ALOUINI (S'94–M'98–SM'03–F'09) was born in Tunis, Tunisia. He received the Ph.D. degree in electrical engineering from the California Institute of Technology (Caltech), Pasadena, CA, USA, in 1998. He was a Faculty Member of the University of Minnesota, Minneapolis, MN, USA, and then Texas A&M University, Qatar, Education City, Doha, Qatar, before joining the King Abdullah University of Science and Technology (KAUST), Thuwal, Makkah, Saudi Arabia, as a Professor of electrical engineering, in 2009. His current research interests include the modeling, the design, and the performance analysis of wireless communication systems.